

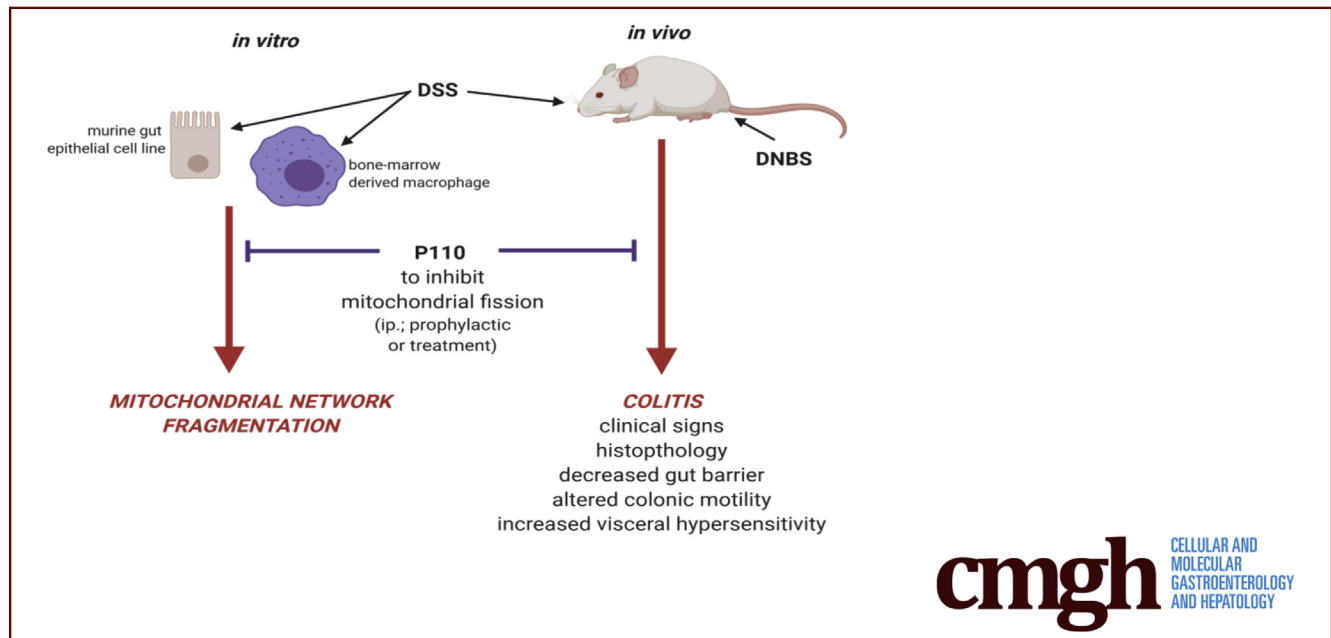
ORIGINAL RESEARCH

Perturbed Mitochondrial Dynamics Is a Novel Feature of Colitis That Can Be Targeted to Lessen Disease



Nicole L. Mancini,^{1,a} Luke Goudie,^{2,a} Warren Xu,² Rasha Sabouny,³ Sruthi Rajeev,¹ Arthur Wang,¹ Nicolas Esquerre,⁴ Ala Al Rajabi,¹ Timothy S. Jayme,¹ Erik van Tilburg Bernandes,^{1,5} Yasmin Nasser,⁴ José G. P. Ferraz,⁴ Timothy Shutt,³ Jane Shearer,⁶ and Derek M. McKay¹

¹Gastrointestinal Research Group (GIRG) and Inflammation Research Network, Department of Physiology and Pharmacology, Calvin, Joan and Phoebe Snyder Institute for Chronic Diseases, Cumming School of Medicine, University of Calgary; ²Department of Biomedical Engineering, Schulich School of Engineering, University of Calgary; ³Department of Medical Genetics, Alberta Children's Hospital Research Institute, University of Calgary; ⁴GIRG, Division of Gastroenterology, Department of Medicine, Cumming School of Medicine, University of Calgary; ⁵Department of Pediatrics, Cumming School of Medicine, University of Calgary; and ⁶Department of Biochemistry and Molecular Biology, Faculty of Kinesiology, University of Calgary, Calgary, Alberta, Canada



SUMMARY

Mitochondrial dysfunction has been described in inflammatory bowel disease. Systemic delivery of P110, a drug designed to prevent fragmentation of the mitochondrial network, significantly reduced the severity of disease (eg, clinical signs, histopathology, and pain) in murine models of colitis.

BACKGROUND & AIMS: Mitochondria exist in a constantly remodelling network, and excessive fragmentation can be pathophysiological. Mitochondrial dysfunction can accompany enteric inflammation, but any contribution of altered mitochondrial dynamics (ie, fission/fusion) to gut inflammation is

unknown. We hypothesized that perturbed mitochondrial dynamics would contribute to colitis.

METHODS: Quantitative polymerase chain reaction for markers of mitochondrial fission and fusion was applied to tissue from dextran sodium sulfate (DSS)-treated mice. An inhibitor of mitochondrial fission, P110 (prevents dynamin related protein [Drp]-1 binding to mitochondrial fission 1 protein [Fis1]) was tested in the DSS and di-nitrobenzene sulfonic acid (DNBS) models of murine colitis, and the impact of DSS ± P110 on intestinal epithelial and macrophage mitochondria was assessed *in vitro*.

RESULTS: Analysis of colonic tissue from mice with DSS-colitis revealed increased mRNA for molecules associated with mitochondrial fission (ie, Drp1, Fis1) and fusion (optic atrophy factor 1) and increased phospho-Drp1 compared with control.

Systemic delivery of P110 in prophylactic or treatment regimens reduced the severity of DSS- or DNBS-colitis and the subsequent hyperalgesia in DNBS-mice. Application of DSS to epithelial cells or macrophages caused mitochondrial fragmentation. DSS-evoked perturbation of epithelial cell energetics and mitochondrial fragmentation, but not cell death, were ameliorated by in vitro co-treatment with P110.

CONCLUSIONS: We speculate that the anti-colitic effect of systemic delivery of the anti-fission drug, P110, works at least partially by maintaining enterocyte and macrophage mitochondrial networks. Perturbed mitochondrial dynamics can be a feature of intestinal inflammation, the suppression of which is a potential novel therapeutic direction in inflammatory bowel disease. (*Cell Mol Gastroenterol Hepatol* 2020;10:287–307; <https://doi.org/10.1016/j.jcmgh.2020.04.004>)

Keywords: inflammation; epithelium; macrophage; DNBS; DSS.

Perturbed gut function can occur in response to mitochondrial dysfunction.^{1,2} Analyses of colitis in mice and epithelial cell culture models of barrier function have provided mechanistic underpinnings for how perturbed mitochondrial activity can contribute to enteric inflammation.^{3–8} Furthermore, abnormal mitochondrial ultrastructure, reduced levels of adenosine triphosphate (ATP) synthase, antioxidants, and Krebs' cycle enzymes, as well as increased oxidative stress have been observed in colonic biopsies from patients with inflammatory bowel disease (IBD).^{9–12} Indeed, a focus on epithelial mitochondrial dysfunction is compatible with the consensus on IBD etiology; disease occurs in genetically susceptible individuals by hyperactive immune responses triggered by environmental stimuli involving the gut microbiota.¹³ In this context, mitochondria are important in the regulation of epithelial permeability,¹⁴ and infection with bacterial pathogens can impair mitochondrial function.^{15,16} Ulcerative colitis has been suggested as a disease of energy deficiency,¹⁷ and in accordance, recent transcriptomic analysis revealed a mitochondriopathy in ulcerative colitis.¹⁸

Mitochondria exist as a network that is constantly remodelling by the processes of fusion and fission that is critical to cellular homeostasis.¹⁹ Fusion facilitates subcellular targeting of ATP and reactive oxygen species (ROS) and equalizes the distribution of proteins, metabolites, and mitochondrial DNA throughout the network.²⁰ Fission allows for mitochondrial partitioning during cell division and the removal of damaged segments of mitochondria by mitophagy; excessive fragmentation of the network can be a stimulus for apoptosis.²¹ The guanosine triphosphatase (GTPase) dynamin family members, dynamin-related protein 1 (Drp1) and optic atrophy factor 1 (OPA1), are major players in mitochondrial fission and fusion, respectively.¹⁹ Imbalanced mitochondrial dynamics play a role in many pathologic conditions including neurodegenerative disease, heart disease, metabolic syndrome, and cancer.^{22,23} All of the aforementioned conditions have an inflammatory component, and yet mitochondrial dynamics are unstudied in the context of enteric inflammation. Furthermore,

blocking excessive fission has proven beneficial in animal models of myocardial infarction, pulmonary arterial hypertension, ischemic-reperfusion injury, multiple sclerosis, and Huntington's disease.^{23–25}

Consequently, we hypothesized that excessive mitochondrial fission would contribute to the pathogenesis of colitis, potentially by resulting in reduced barrier function and reduced viability of the epithelium. After uncovering evidence for altered mitochondrial dynamics in tissues from mice with colitis, systemic administration of a selective inhibitor of fission, P110 (inhibits Drp1 binding to mitochondrial fission 1 protein [Fis1])²⁵ reduced disease severity in dextran sodium sulfate (DSS)- or dinitrobenzene sulfonic acid (DNBS)-treated mice. Furthermore, DSS induced fragmentation of macrophage and gut epithelial mitochondria in vitro, and the accompanying reduction in bioenergetics in the latter was partially abrogated by co-treatment with P110. These data suggest that perturbed mitochondrial dynamics in enterocytes and macrophages could be a component of enteric inflammatory disease, and that reducing mitochondrial dysfunction due to excessive fragmentation could promote intestinal homeostasis in individuals who show evidence of enhanced mitochondrial fission.

Results

Quantitative Polymerase Chain Reaction Indicates Altered Expression of Mitochondrial Dynamics Molecules in Colitis

Quantitative polymerase chain reaction (qPCR) on murine colonic tissue revealed increased expression of mRNA for Drp1, Fis1, OPA1, mitofusin (MFN) 1, and MFN2 by 5 days after exposure to DSS (Figure 1A–E). Immunoblotting revealed an increase in phospho-Ser616 Drp1 (a stimulus for Drp1 to translocate to mitochondria) in tissue extracts from mice treated with DSS for 5 days (Figure 1F and G).

Systemic Administration of P110 Reduces Disease Severity in Murine Models of Colitis

P110 is a selective inhibitor of Drp1-Fis1 driven mitochondrial fission.²⁴ P110 (1 μmol/L) activity was confirmed in vitro by its ability to reduce Drp1 recruitment to mitochondria and ROS generation by carbonyl cyanide

^aAuthors share co-first authorship.

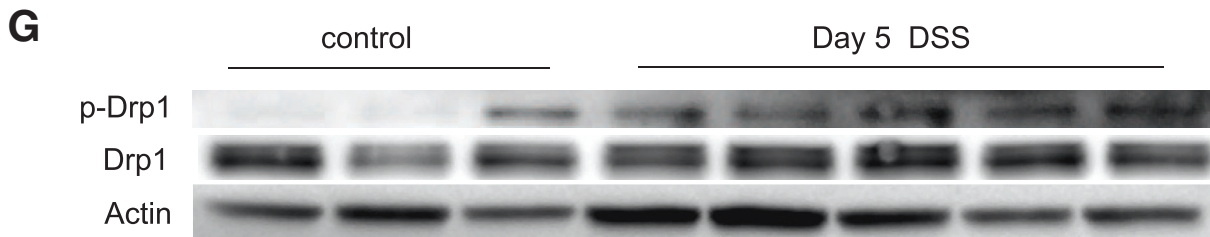
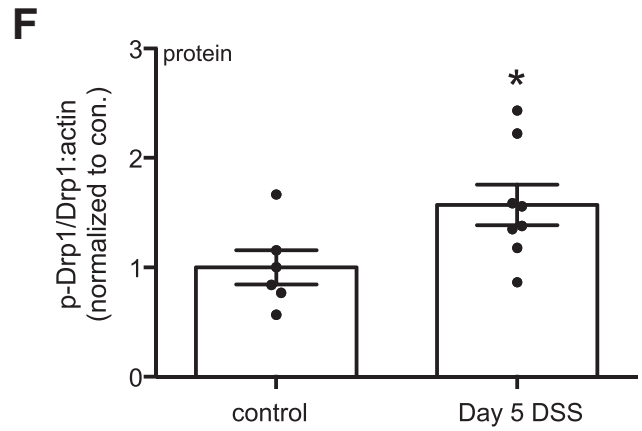
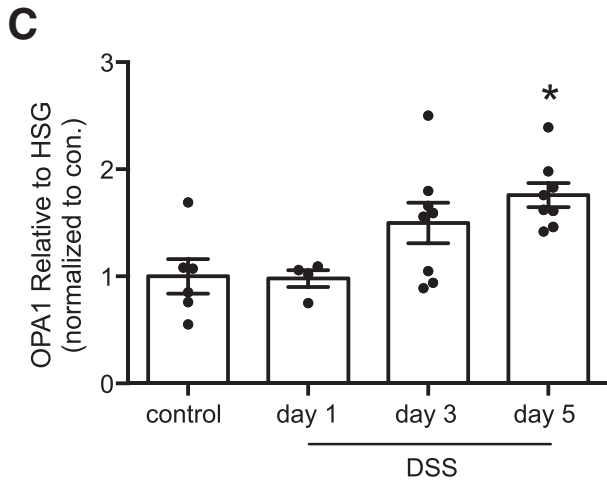
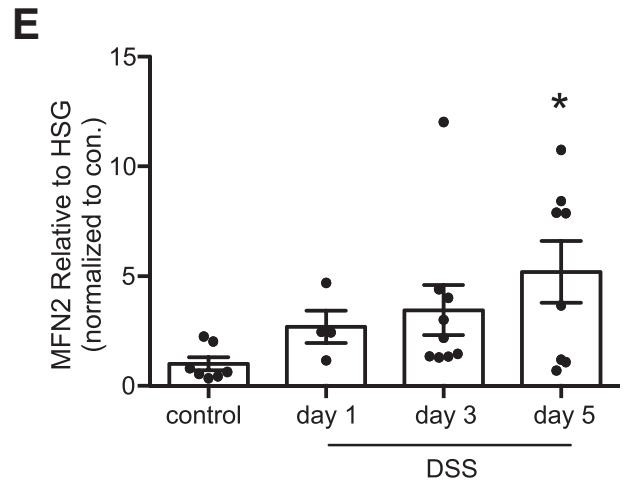
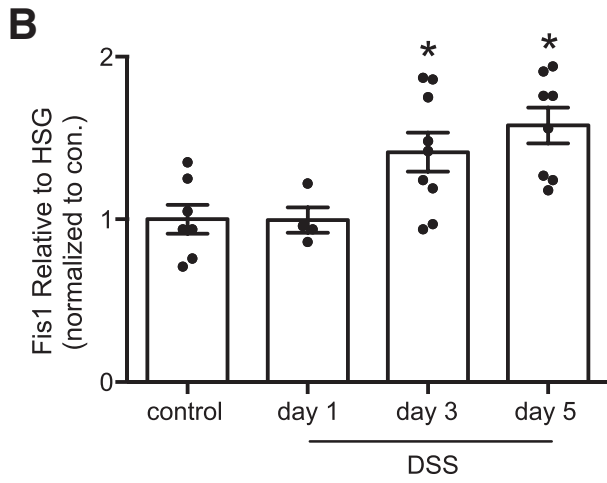
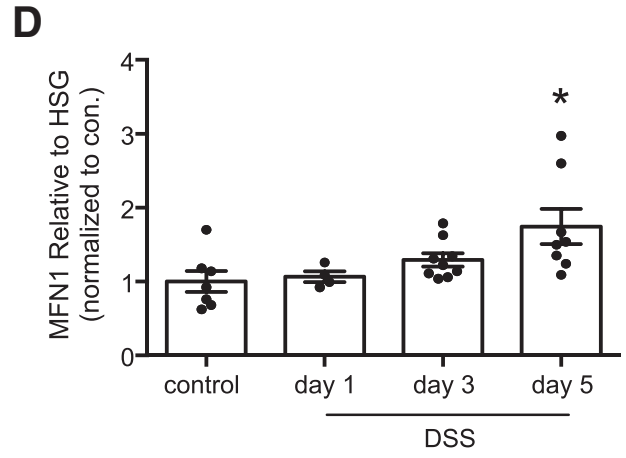
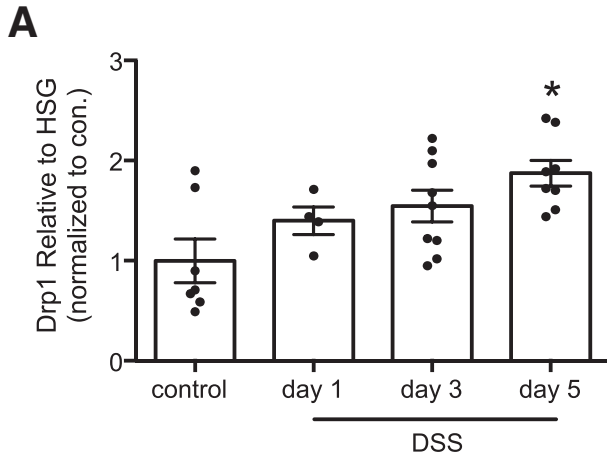
Abbreviations used in this paper: ATP, adenosine triphosphate; DNBS, di-nitrobenzene sulfonic acid; Drp1, dynamin related protein-1; DSS, dextran sodium sulfate; Fis1, mitochondrial fission protein-1; GM-CSF, granulocyte-macrophage colony-stimulating factor; GTPase, guanosine triphosphatase; IBD, inflammatory bowel disease; IEC, intestinal epithelial cell; IL, interleukin; LPS, lipopolysaccharide; MFN, mitofusin; OPA1, optic atrophy factor 1; qPCR, quantitative polymerase chain reaction; ROS, reactive oxygen species; TER, transepithelial electrical resistance; TNF, tumor necrosis factor; TUNEL, deoxyuride-5'-triphosphate biotin nick end labeling.

 Most current article

© 2020 The Authors. Published by Elsevier Inc. on behalf of the AGA Institute. This is an open access article under the CC BY-NC-ND license (<http://creativecommons.org/licenses/by-nc-nd/4.0/>).

2352-345X

<https://doi.org/10.1016/j.jcmgh.2020.04.004>



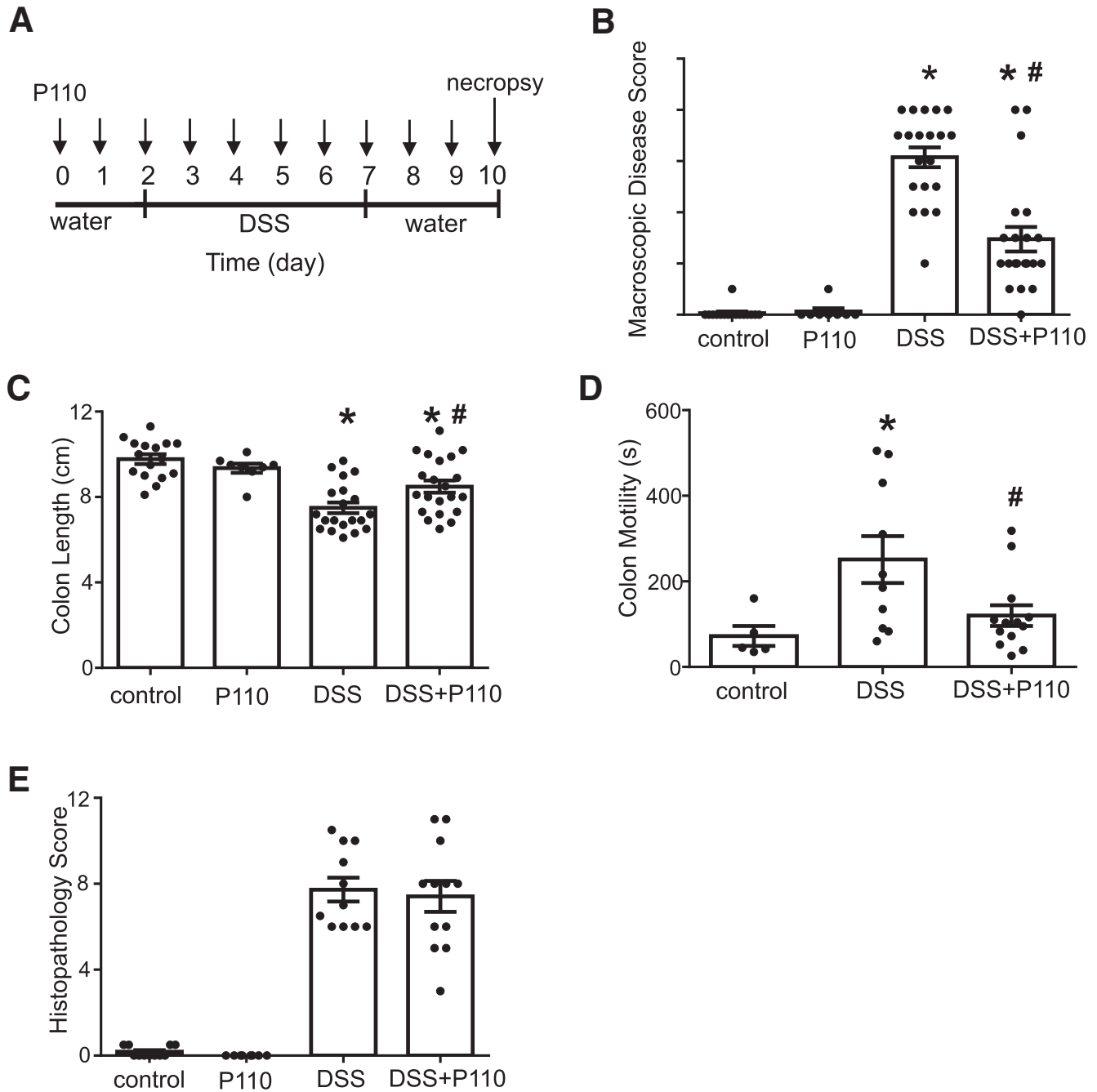


Figure 2. Systemic administration of P110 reduces severity of DSS-induced colitis. (A) Male BALB/c mice were given 5% DSS drinking water for 5 days, followed by 3-day water recovery phase \pm daily P110 (intraperitoneal; 3 mg/kg) as shown. On necropsy, (B) macroscopic disease activity scores were calculated, (C) colon length was measured, and (D) just before necropsy, colonic motility was assessed in anesthetized animals (s, seconds). (E) Histopathology scoring was performed on H&E stained sections of mid-colon in a blinded fashion (mean \pm standard error of the mean; $n = 8$ –21 mice from 2 to 5 experiments; $*P < .05$ compared with control, $\#P < .05$ compared with DSS; (B and E) Kruskal-Wallis and then Dunn multiple comparison test; (C and D) one-way analysis of variance and then Tukey multiple comparison test.

Figure 1. (See previous page). Colitis evokes increased expression of mRNA of molecules that regulate mitochondrial dynamics. (A–E) qPCR performed on segments of colonic tissue from DSS (5%) treated male BALB/c mice revealed increased expression of Drp1, mitochondrial Fis1, OPA1, and MFN1 and MFN2 mRNA (data normalized to 18S rRNA as a housekeeping gene [HSG]). Expression levels in each tissue extract were compared with the mean of the control group that was set at 1 ($*P < .05$ compared with control; one-way analysis of variance, Dunnett multiple comparison test). (F) Densitometric analysis for phosphorylated Drp1 (p-Drp1 Ser616):total Drp1 ration normalized to actin in murine colonic extracts (day 5, 5% DSS), with (G) illustrating a representative immunoblot (mean \pm standard error of the mean; $*P < .05$, t test) (each dot represents an individual mouse).

m-chlorophenyl hydrazine (10 $\mu\text{mol/L}$) treatment of T84 epithelial cells (data not shown; $n = 4$). Mice treated with the TAT protein only (data not shown) or P110 only (Figure 2) showed no signs of ill health, whereas DSS-treated mice had shortened colons, increased macroscopic disease scores, increased colonic transit time, and histopathology (ie, loss of architecture, goblet cell depletion, inflammatory cell infiltration, and ulceration) (Figure 2). Macroscopic disease scores were reduced by $\sim 50\%$ in the DSS + P110 group compared with DSS (Figure 2B), and mice receiving P110 had a longer colon and colonic transit time not different from control mice (Figure 2C and D). In contrast, colonic histopathology was not appreciably different between DSS- and DSS + P110-treated mice (Figure 2E). Bacterial dysbiosis occurred in DSS-treated mice, and this was unaffected by co-treatment with P110 (Table 1, Figure 3).

Treatment of BALB/c mice with DNBS resulted in severe colitis, with $\sim 21\%$ of mice (5/24) reaching a predetermined ill health endpoint requiring euthanasia (Figure 4A and B). Systemic delivery of P110 in a prophylactic regimen resulted in less weight loss (Figure 4C), with only 1 mouse of 27 (1%) requiring euthanasia (Figure 4B). Similarly, the P110-treated mice had longer colons and lower disease activity scores compared with DNBS-only treated mice (Figure 4D and E). Mice treated with DNBS + P110 had significantly less colonic histopathology, displaying improved architecture and crypt morphology and reduced inflammatory cell infiltrate (Figure 4F and G). Positive deoxyuride-5'-triphosphate biotin nick end labeling (TUNEL) staining mirrored the damage observed on H&E sections, with numerous dead cells (and debris) throughout sections from DNBS-treated mice and less so in the DNBS + P110 group (Figure 4G). Assessment of epithelial proliferation revealed Ki67⁺ cells toward the base of crypts in control tissue, and this extended further up the crypt in sections from DNBS + P110-treated mice, likely reflecting ongoing tissue regeneration/recovery after the pro-colitic

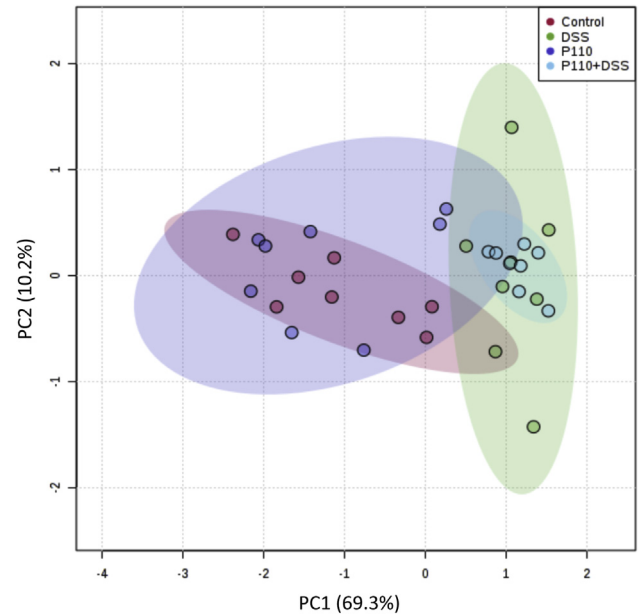


Figure 3. P110 treatment does not correct DSS-induced dysbiosis. To discern changes to the bacterial population caused by DSS \pm P110 (Figure 2), total DNA was extracted from fecal/cecal samples and analyzed with qPCR for 16S rRNA copy number. Data were assessed by Metaboanalyst 4.0, and principal component analysis (PCA) was plotted. Each dot represents data from an individual animal, and area outlined in corresponding color depicts the 95% confidence region. P110 only did not alter bacterial composition as compared with control and did not affect dysbiosis caused by DSS.

stimulus (Figure 4G). Colon from DNBS-treated mice had increased granulocyte-macrophage colony-stimulating factor (GM-CSF), interleukin (IL) 6, and tumor necrosis factor (TNF) α protein, the levels of which were lower in colon from DNBS + P110-treated mice (Figure 5A). In addition, P110 treatment improved gut barrier function as assessed

Table 1. Analysis of Fecal/Cecal Bacterial Composition in Dextran Sodium Sulfate-Treated Mice \pm Systematic Treatment With the P110 Inhibitor of Mitochondrial Fission

Treatment	Control	P110	DSS	DSS + P110
Bacteroides	6.54 \pm 0.08	6.64 \pm 0.07	6.77 \pm 0.08 ^a	6.80 \pm 0.07 ^a
<i>Clostridium coccooides</i> (cluster XIV)	6.50 \pm 0.09	6.50 \pm 0.06	6.22 \pm 0.09 ^a	6.25 \pm 0.08 ^a
<i>Clostridium leptum</i> (cluster IV)	5.71 \pm 0.06	5.78 \pm 0.80	5.22 \pm 0.10 ^a	5.23 \pm 0.06 ^a
<i>Clostridium</i> cluster XI	1.68 \pm 0.06	1.33 \pm 0.08	1.53 \pm 0.08	1.50 \pm 0.16
<i>Clostridium</i> cluster I	1.50 \pm 0.11	1.51 \pm 0.10	1.08 \pm 0.15 ^a	0.97 \pm 0.10 ^a
<i>Roseburia hominis</i>	2.75 \pm 0.19	2.81 \pm 0.31	1.38 \pm 0.08 ^a	1.35 \pm 0.04 ^a
<i>Faecalibacterium prausnitzii</i>	3.68 \pm 0.19	3.87 \pm 0.30	2.30 \pm 0.08 ^a	2.29 \pm 0.04 ^a
<i>Lactobacillus</i> spp.	1.76 \pm 0.08	1.78 \pm 0.12	1.51 \pm 0.09 ^a	1.56 \pm 0.09 ^a
<i>Bifidobacterium</i> spp.	3.63 \pm 0.08	3.79 \pm 0.04	3.54 \pm 0.09 ^a	3.49 \pm 0.08 ^a
<i>Methanobrevibacter</i> spp.	2.02 \pm 0.11	1.95 \pm 0.05	1.94 \pm 0.08	1.88 \pm 0.11
Enterobacteriaceae	2.15 \pm 0.11	2.17 \pm 0.10	1.74 \pm 0.15 ^a	1.63 \pm 0.10 ^a
<i>Akkermansia muciniphila</i>	1.72 \pm 0.18	2.02 \pm 0.10	1.57 \pm 0.25	1.41 \pm 0.19

NOTE. Data are mean 16S RNA gene/mg fecal-cecal material \pm standard error of the mean; $n = 4$ samples/group.
^a $P < .05$ compared with controls.

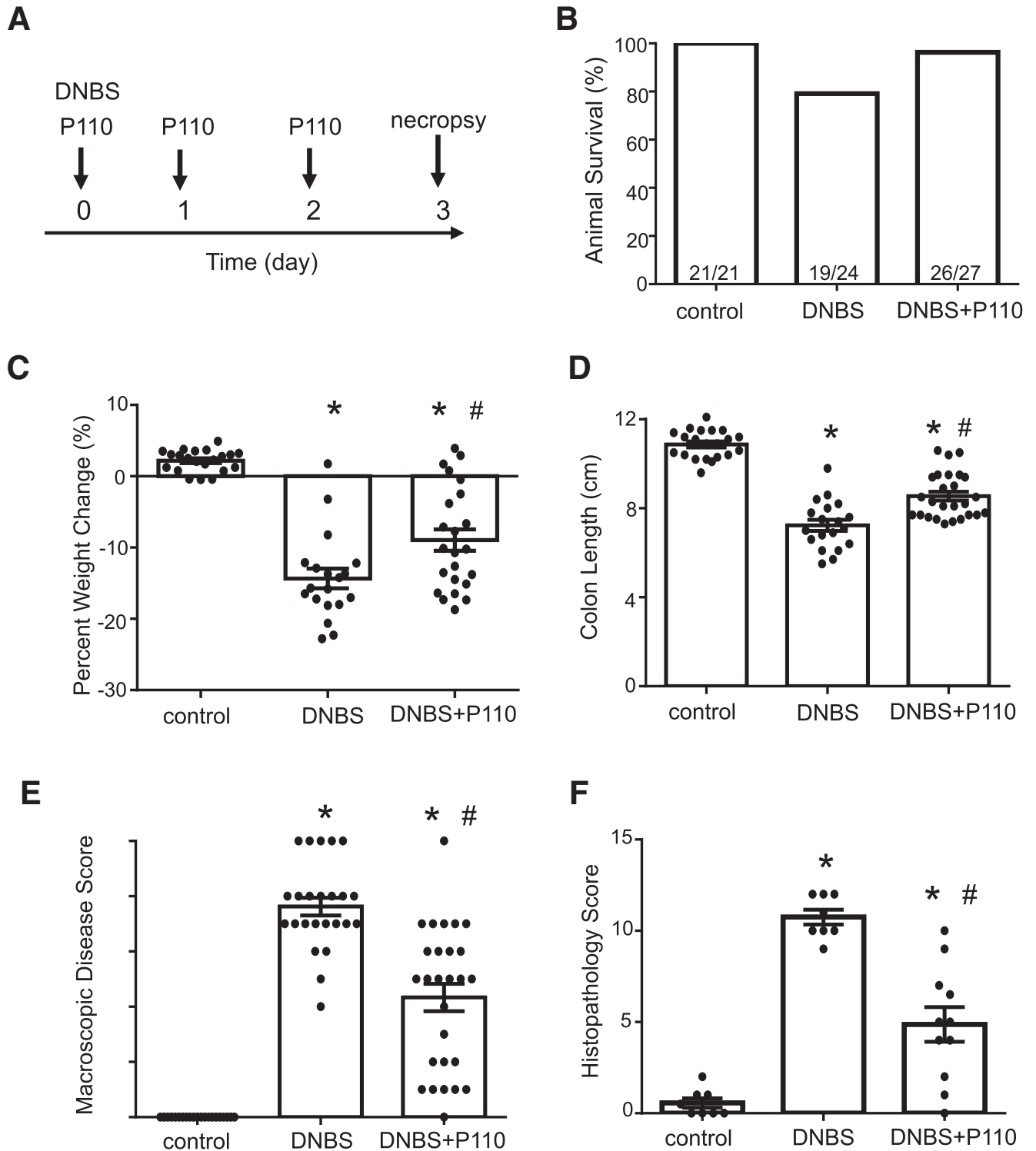


Figure 4. Prophylactic administration of P110 reduces severity of DNBS-induced colitis. Male BALB/c mice were treated with DNBS (3 mg, intrarectal) ± P110 (intraperitoneal, 3 mg/kg) as shown in (A). (B) and (C) Numbers of mice requiring humane euthanasia because of disease severity and daily weight change, respectively. On necropsy, colon length was measured (D), macroscopic disease score was calculated (E), and a piece of mid-colon was processed for H&E staining and assessment of histopathology in a blinded fashion (F) (mean ± standard error of the mean; n = 11–27 mice from 3 to 6 experiments). (G) Representative histologic images of the colon stained with H&E, an antibody against the proliferation-associated antigen, Ki67, and the TUNEL assay for apoptosis (n = 9–11 mice, 2 experiments; m, muscle; c, crypt; l, lumen; *, inflammatory cell infiltrate; arrowhead, dead cells; scale bar = 50 μm) (*P < .05 compared with control, #P < .05 compared with DNBS; (C) and (D) one-way analysis of variance and then Tukey multiple comparison test; (E) and (F) Kruskal-Wallis and then Dunn multiple comparison test.

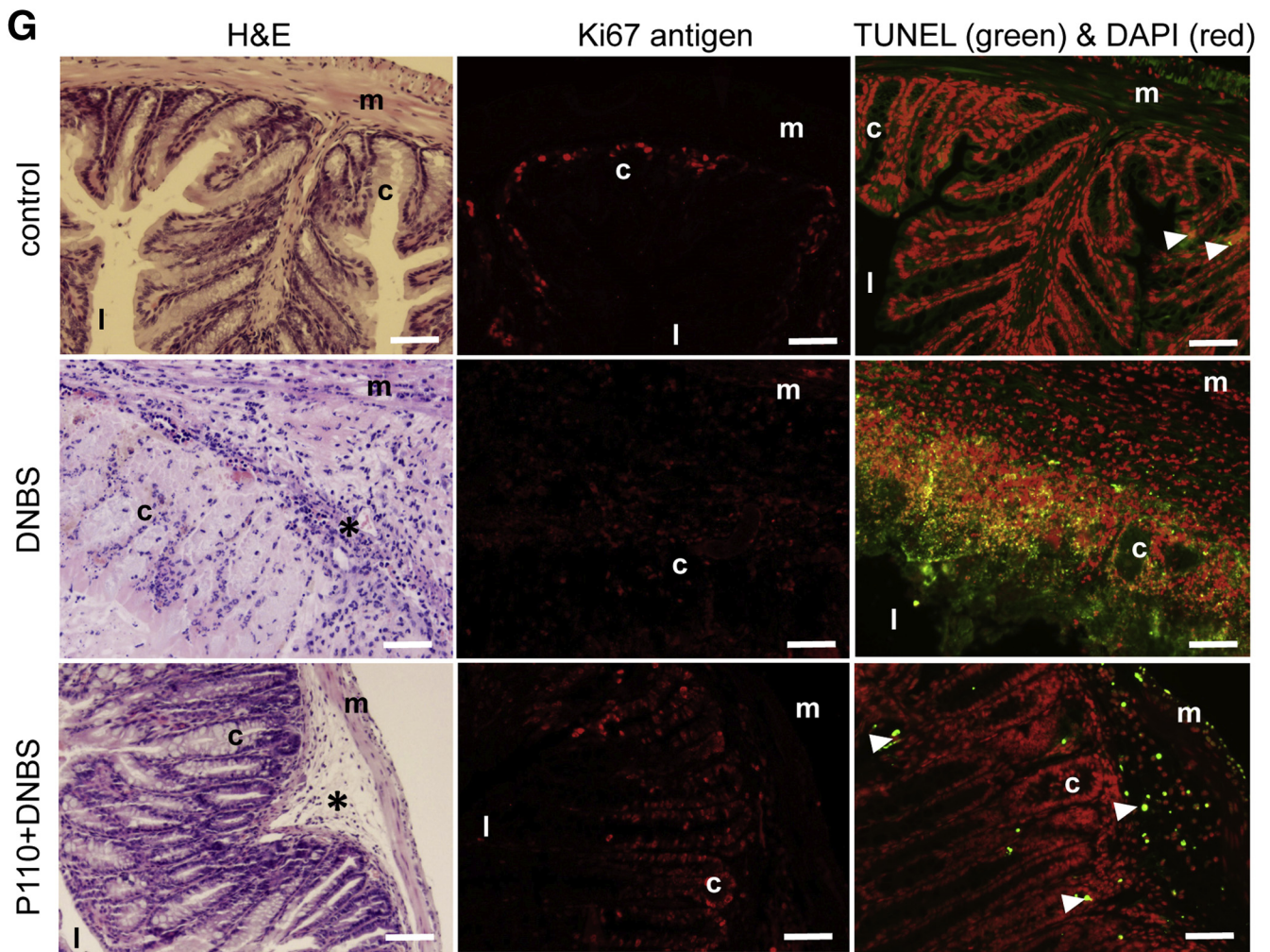


Figure 4. (continued).

by lumen-to-blood movement of fluorescein isothiocyanate-dextran, whereas detection of aerobic bacteria in liver and splenic extracts was only observed in the DNBS group of mice (Figure 5B).

DNBS-colitis spontaneously resolves, and by 7 days after treatment, mice display normal behavior and milder colitis.²⁶ Using P110 in a treatment regimen (Figure 6A) resulted in improved disease recovery; none of the treated animals required euthanasia (Figure 6B), weight loss was reduced (Figure 6C), colons were longer, and macroscopic disease scores were lower (Figure 6D and E) than in DNBS-only treated mice. Histologic analysis showed normal morphology in sections from control mice, with some TUNEL⁺ cells in the apical epithelium and Ki67 staining restricted to the base of crypts (Figure 6G). Colon from DNBS-treated mice was characterized by focal ulceration, inflammatory cell infiltrate, and patches of deranged crypt structure and increased TUNEL staining in the epithelium, mucosa, and into the submucosa; Ki67 staining was dispersed throughout areas of tissue damage (Figure 6G). In terms of histopathology, cell death (TUNEL⁺), and proliferation (ie, Ki67⁺), tissues from DNBS + P110-treated mice

displayed less damage than DNBS-only treated mice and evidence of crypt elongation and increased Ki67⁺ cells suggestive of tissue regeneration. Comparable with P110 used in the prophylactic regimen, GM-CSF, IL6, and TNF α protein levels were reduced in colon from mice treated with DNBS + P110 as a treatment compared with DNBS-only treated mice (Figure 7A). Consistent with other studies,²⁷ colonic distention to 60 mm Hg pressure had only a minimal effect in control male BALB/c mice. In contrast, mice displayed an obvious hyperalgesia at distention pressures of 45 and 60 mm Hg at 7 days after DNBS, and this was completely abrogated by P110 treatment (Figure 7B).

Analysis of blood smears revealed an increase in neutrophils in DSS- or DNBS-treated mice, and this was unaffected by P110 (data not shown, n = 8).

P110 Blocks Dextran Sodium Sulfate-Induced Mitochondrial Changes in Epithelial Cells and Macrophages

Consistent with previous reports,^{6,28} 2% DSS (24 hours) reduced viability of in vitro cultured epithelial cells as

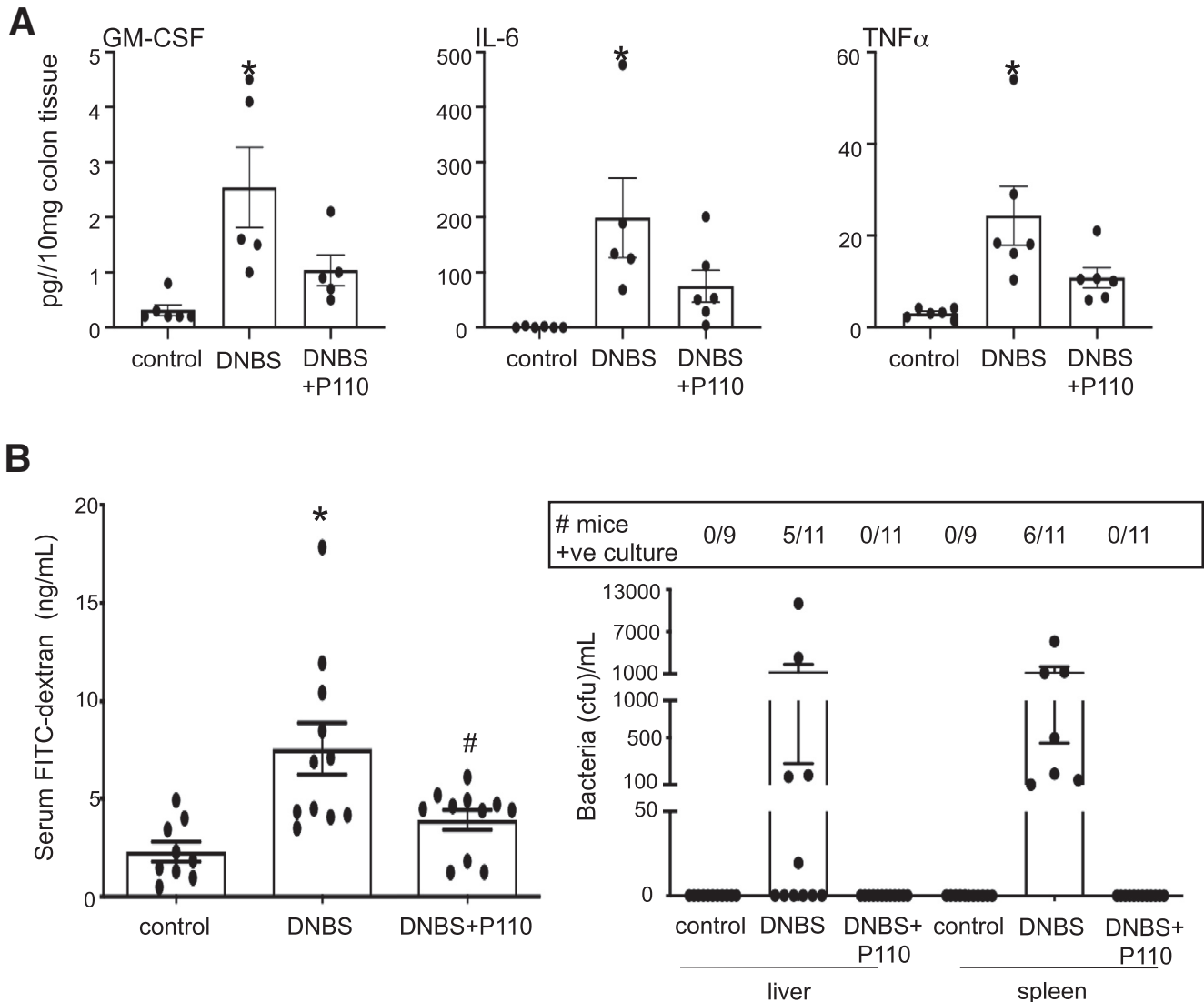


Figure 5. Prophylactic administration of P110 reduces the DNBS-induced increases in gut permeability. (A) Male BALB/c mice were treated as in Figure 4A, and on necropsy ~1-cm pieces of mid-colon were extracted and cytokines were measured ($n = 5-6$). (B) In other mice, gut permeability was assessed by lumen-to-serum movement of fluorescein isothiocyanate-dextran (4 kDa) and number of mice positive (and bacterial colony-forming units) for bacterial anaerobic culture from liver and spleen ($n = 9-11$ mice, 2 experiments) ($*P < .05$ compared with control, $\#P < .05$ compared with DNBS; one-way analysis of variance and then Tukey multiple comparison test; DNBS at 3 mg, intrarectal; P110 at 3 mg/kg, intraperitoneal).

determined by trypan blue exclusion, and this was not affected by P110 co-treatment (Figure 8A). However, the reduced alamarBlue metabolism in DSS-treated cells, indicating reduced nicotinamide adenine dinucleotide (NAD) concentration, was abrogated by P110 co-treatment (Figure 8B), suggesting that the surviving cells were healthier with increased NAD production compared with DSS-only treated enterocytes.

DSS-treated epithelia had an increased percentage of cells with a highly fragmented mitochondrial network, and P110 partially abrogated this effect, resulting in a significant increase in epithelial cells with a mitochondrial network intermediate between fused and fragmented (Figure 8C and E). Similarly, P110 largely abrogated the mitochondrial

fragmentation in bone marrow-derived macrophages treated with 1% DSS for 24 hours (Figure 8D and E) (when treated with 2% DSS, macrophages lost adherence, and those remaining were small and rounded).

To examine the functional impact of P110 on mitochondrial bioenergetics, the oxygen consumption rates of saturating concentrations of specific substrates were assessed after 24 hours of exposure to DSS. Analysis of basal respiration revealed DSS impaired respiration in intestinal epithelial cell (IEC) 4.1 epithelia, which was partially restored with P110 treatment (Figure 9A). Stimulation of electron transport chain complexes I, II, and IV demonstrated that co-treatment with DSS + P110 increased complex IV activity (Figure 9B-D). Trends toward reduced mitochondrial capacity in complex I

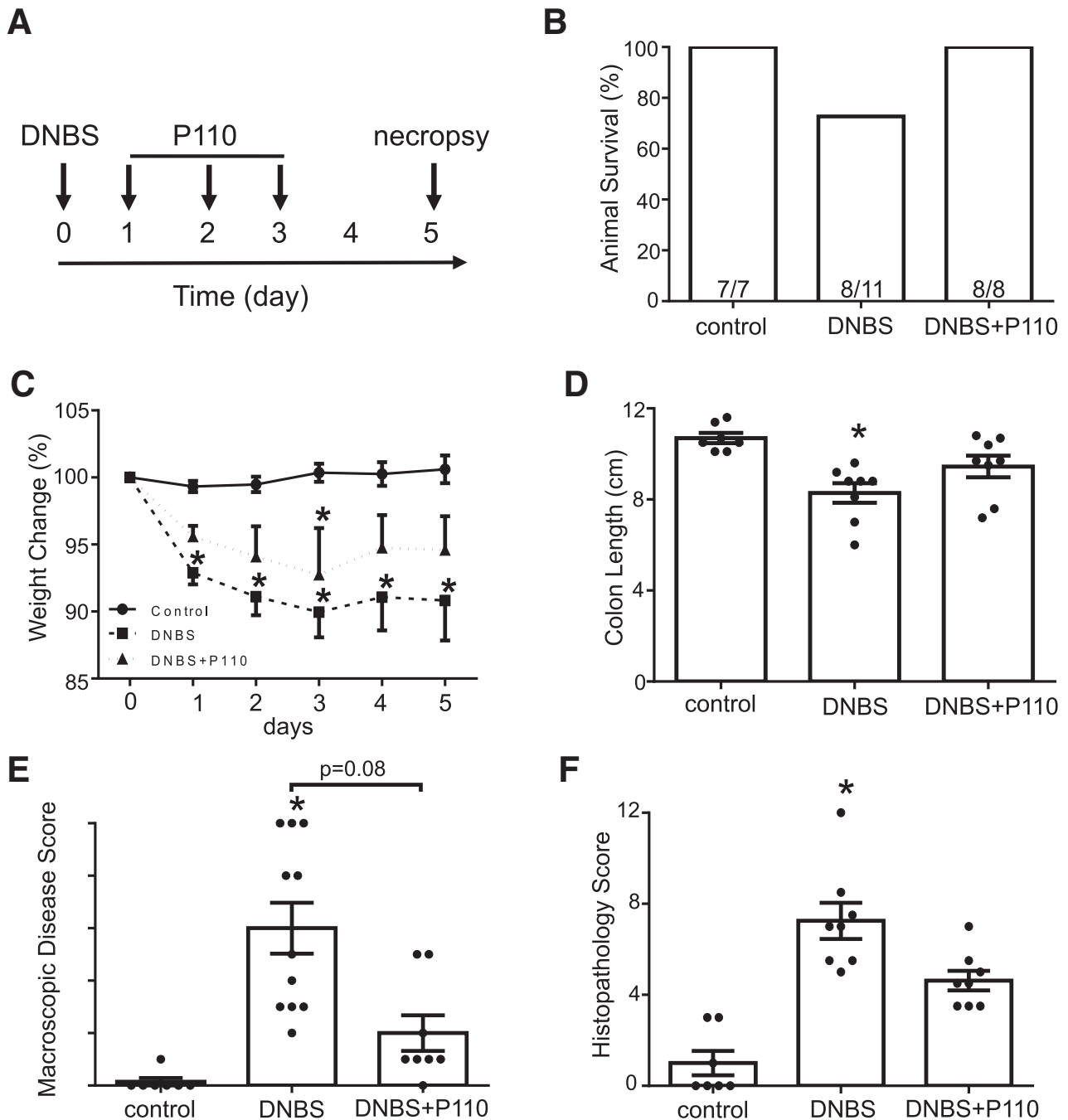


Figure 6. P110 in a treatment protocol reduces the severity of DNBS-induced colitis. (A) Male BALB/c mice were treated with DNBS (3 mg, intrarectal) ± P110 (intraperitoneal, 3 mg/kg). (B) and (C) Numbers of mice requiring humane euthanasia because of disease severity and daily weight change, respectively. On necropsy, colon length was measured (D), macroscopic disease score was calculated (E), and a piece of mid-colon was processed for H&E staining and assessment of histopathology in a blinded fashion (F). (G) Representative histologic images of the colon stained with H&E, an antibody against the proliferation-associated antigen, Ki67, and the TUNEL assay for apoptosis (*m*, muscle; *c*, crypt; *l*, lumen; *arrowhead*, dead cells; scale bar = 50 μ m) (mean \pm standard error of the mean; $n = 7$ –11 mice from 2 experiments; * $P < .05$ compared with control); (C) and (D) one-way analysis of variance and then Tukey multiple comparison test; (E) and (F) Kruksal-Wallis and then Dunn multiple comparison test.

and II in DSS-treated cells were also noted and less so with DSS + P110-treated cells. Epithelial fatty acid oxidation with both short-chain (butyrate) and long-chain fatty acid (palmitate) revealed impairments with DSS that were

abrogated by P110 (Figure 9E and F). These findings show significant metabolic stress in DSS-treated epithelia, and that the perturbed bioenergetics were relieved at least in part by treatment with P110.

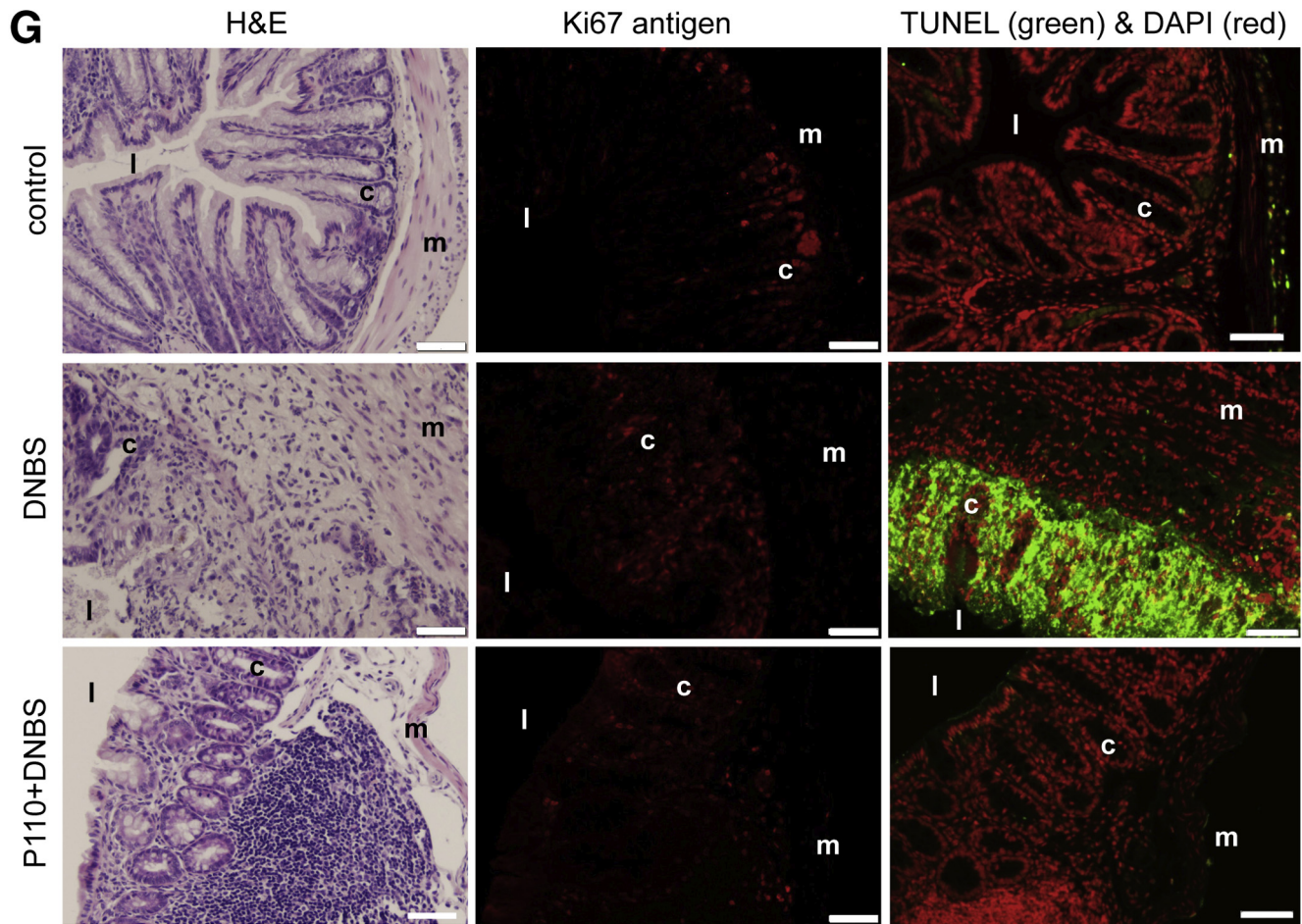


Figure 6. (continued).

P110 Does Not Affect Dextran Sodium Sulfate–Evoked Increased Paracellular Epithelial Permeability In Vitro

Twenty-four hours and 48 hours after exposure to 2% DSS, T84 cell monolayer transepithelial electrical resistance (TER) was reduced by ~20% and ~60%, respectively. This reduction in TER was unaffected by co-treatment with P110 ($n = 10$ monolayers from 3 experiments; data not shown). However, the early drop in TER was prevented by co-treatment with the pan-caspase inhibitor Z-VAD, which also reduced the barrier defect observed at 48 hours after treatment (TER: DSS, $64.5\% \pm 5\%$ ($n = 10$) vs DSS + ZVAD, $80\% \pm 10\%$ ($n = 6$) of pretreatment values; mean \pm standard error of the mean; starting TERs were $1000\text{--}2000 \Omega\text{cm}^2$).

Inhibitors of Mitochondrial Fission Do Not Affect Dextran Sodium Sulfate or Lipopolysaccharide–Evoked Cytokine Production

Epithelia treated with DSS showed a trend toward decreased keratinocyte chemoattractant production, whereas macrophages displayed only small increases in TNF α and IL10 on in vitro exposure to DSS. These responses

were not significantly affected by co-treatment with inhibitors of fission, except for a small increase in IL10 output from 1% DSS + P110-treated macrophages compared with DSS alone (Table 2). Lipopolysaccharide (LPS)-stimulated cytokine production was unaffected by co-treatment with P110 (Table 2).

Discussion

Tremendous advances have been made in treating IBD, yet many patients are or become refractory to biologic therapy, the gold standard therapy²⁹; hence there is the imperative to explore novel targets to treat IBD. A body of data demonstrates perturbed mitochondrial activity in IBD, and mitochondrial malfunction can result in gastrointestinal symptoms.³⁰ However, the role that dysfunctional mitochondria in the enteric epithelium, or other gut cells, plays in the pathophysiology of IBD is unclear. A few studies suggest that targeting mitochondria could be valuable in treating enteric inflammation.^{6,18,31–33}

Mitochondrial function has been described in murine models of colitis. Mitochondrial dysfunction in DSS-colitis is supported by subtle reductions in the mitochondria-specific voltage-dependent anion channel,⁶ lower tissue levels of ATP, and a less complex mitochondrial network.⁸ Also,

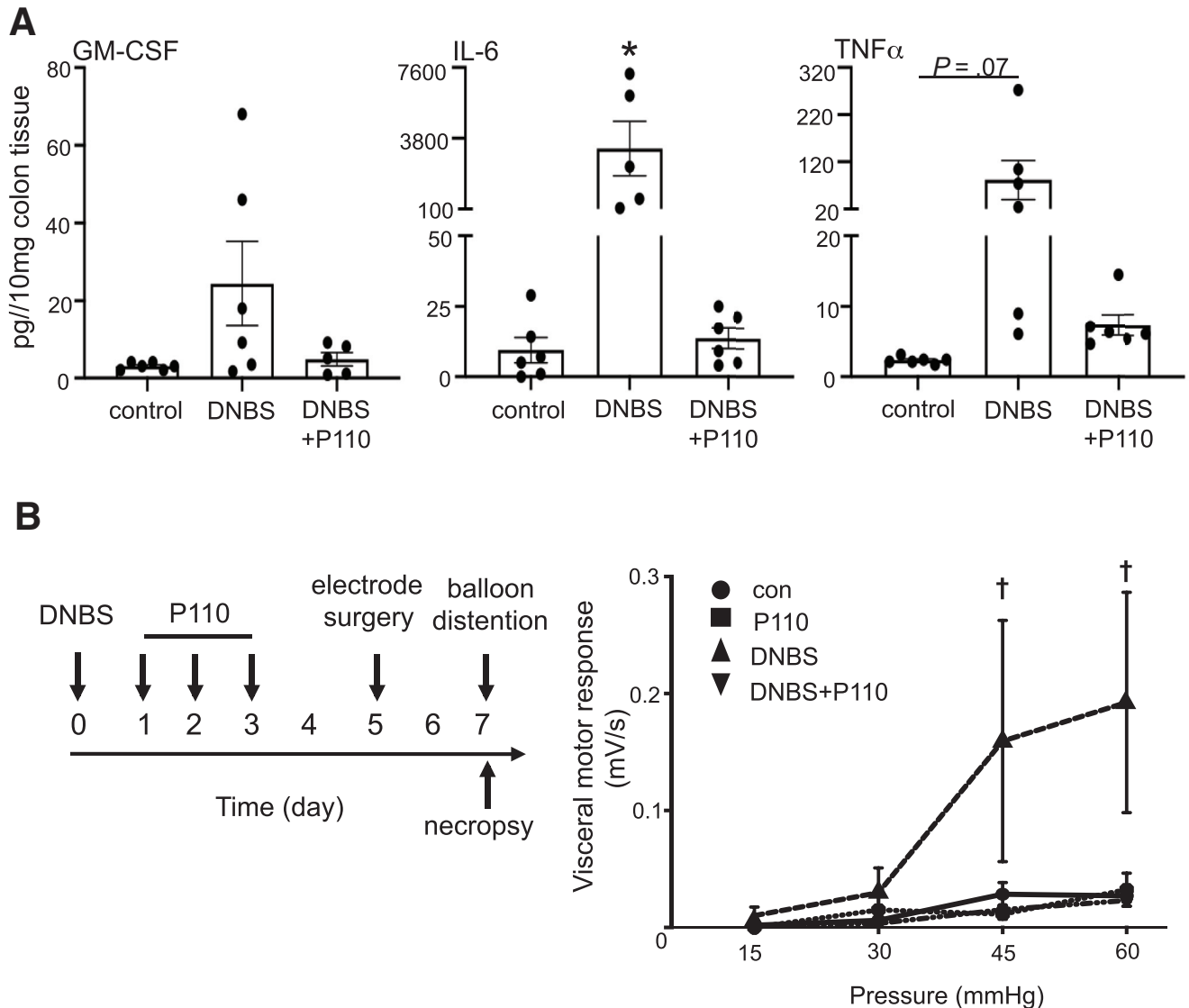


Figure 7. P110 in a treatment protocol reduces colonic cytokine levels and pain perception in DNBS-treated mice. (A) Male BALB/c mice were treated as in Figure 6A, and on necropsy ~1-cm pieces of mid-colon were extracted and cytokines were measured ($n = 5-6$; $*P < .5$ compared with control). (B) Treatment regimen (left) and the hyperalgesia response recorded in DNBS-treated mice with colonic distention of 45 and 60 mm Hg pressure that was prevented by P110 co-treatment ($n = 10-13$ mice, 2 experiments); ($\dagger P < .05$ compared with DNBS only; Kruskal-Wallis and then Dunn multiple comparison test; DNBS at 3 mg intrarectal; P110 at 3 mg/kg intraperitoneal).

mutation in the multidrug resistance 1 gene is a susceptibility trait for ulcerative colitis, and *mdr1*^{-/-} mice present with damaged epithelial mitochondria⁴ (as can trinitrobenzene sulfonic acid-treated rats³⁴). The “health” of the mitochondrial network is a key aspect of cellular homeostasis, where excessive fission or reduced fusion is implicated in many diseases.²³ Exposure to DSS resulted in increased Drp1, Fis1, OPA1, MFN1, and MFN2 mRNA, and increases in phospho-Ser616 activated Drp1 in murine colonic tissue. This finding suggests perturbed mitochondrial dynamics in the colitic tissue. Future studies enabled by enhanced in situ imaging should assess epithelial mitochondrial network morphology in colonic tissue. These data beg the question whether use of an inhibitor of mitochondrial fission would be beneficial in enteric inflammation.

Pharmacologic options to block mitochondrial fission in vivo are limited. Mdivi1 blocks the GTPase activity of Drp1 but may have off-target effects related to oxidative phosphorylation and the suppression of ROS.³⁵ The anti-rheumatic drug, leflunomide, blocks pyrimidine synthesis and was recently shown to antagonize mitochondrial fission by promoting fusion.³⁶ The small peptide P110 is conjugated to the HIV-TAT protein to facilitate transduction into cells and was designed to block Fis1-Drp1 interaction, thus reducing fission.²⁴ Because of increased Drp1 and Fis1 mRNA expression in DSS-treated mice, P110 was a rational choice to test for putative anti-colitic efficacy in animal models of colitis.

Systemic delivery of P110 significantly reduced the severity of murine colitis; the mice displayed fewer

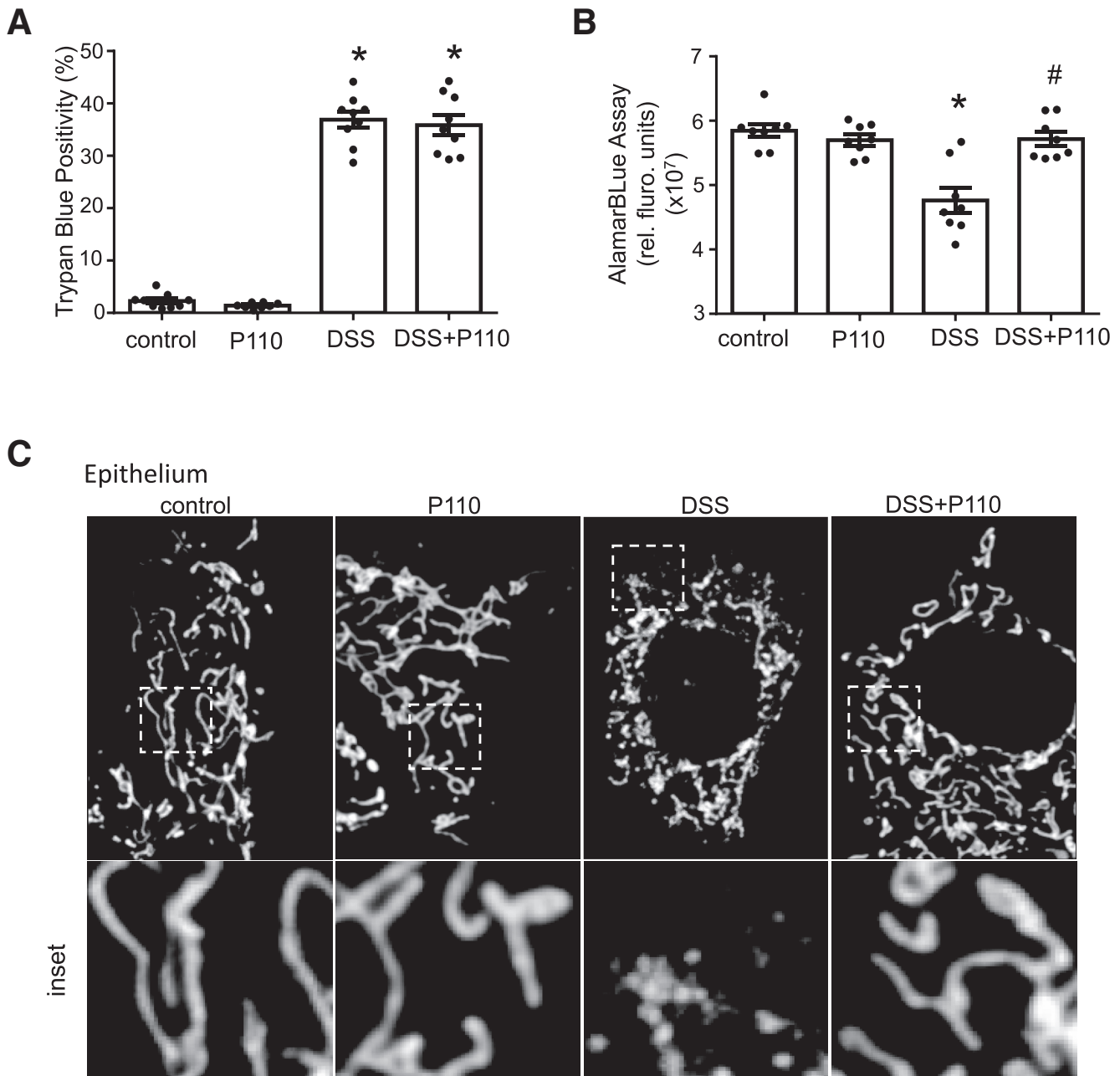


Figure 8. Treatment with P110 reduced DSS-induced epithelial and macrophage mitochondrial fragmentation. (A) DSS (2%, 24 hours) applied to cells of the murine IEC^{4.1} epithelial cell line is cytotoxic as gauged by increased trypan blue staining that is not affected by P110 (1.5 $\mu\text{mol/L}$) co-treatment, whereas the reduced mitochondrial activity (alamarBlue cleavage indicating reduced nicotinamide adenine dinucleotide concentration) caused by DSS was blocked by P110 (B). Mitochondrial networks (representative images shown in (C) [epithelial] and (D) [macrophage]) were quantified in the murine small intestinal epithelial IEC 4.1 cell line and murine bone marrow–derived macrophages (E) and designated as predominantly fused, fragmented, or intermediate (20 cells from each epithelial or macrophage preparation was assessed) (data are mean \pm standard error of the mean; $n = 6$ epithelial and $n = 4$ macrophage preparations; * $P < .05$ compared with control, # $P < .05$ compared with DSS, two-way analysis of variance, Tukey multiple comparison test).

macroscopic signs of disease, colonic dysmotility was normalized, and in the DNBS model, improved gut barrier function and reduced colonic levels of GM-CSF, IL6, and TNF α were apparent. Moreover, only 1 of 35 mice (3%) treated with DNBS + P110 (data combined from treatment and prophylactic regimens) required humane

euthanasia, whereas 8 of 35 (~23%) DNBS-only treated mice developed severe illness requiring euthanasia. Visceral pain was assessed, and strikingly, the colonic hyperalgesia that characterized DNBS-colitis was absent in DNBS + P110-treated mice. Although this may reflect reduced inflammation in the colon, it is also compatible

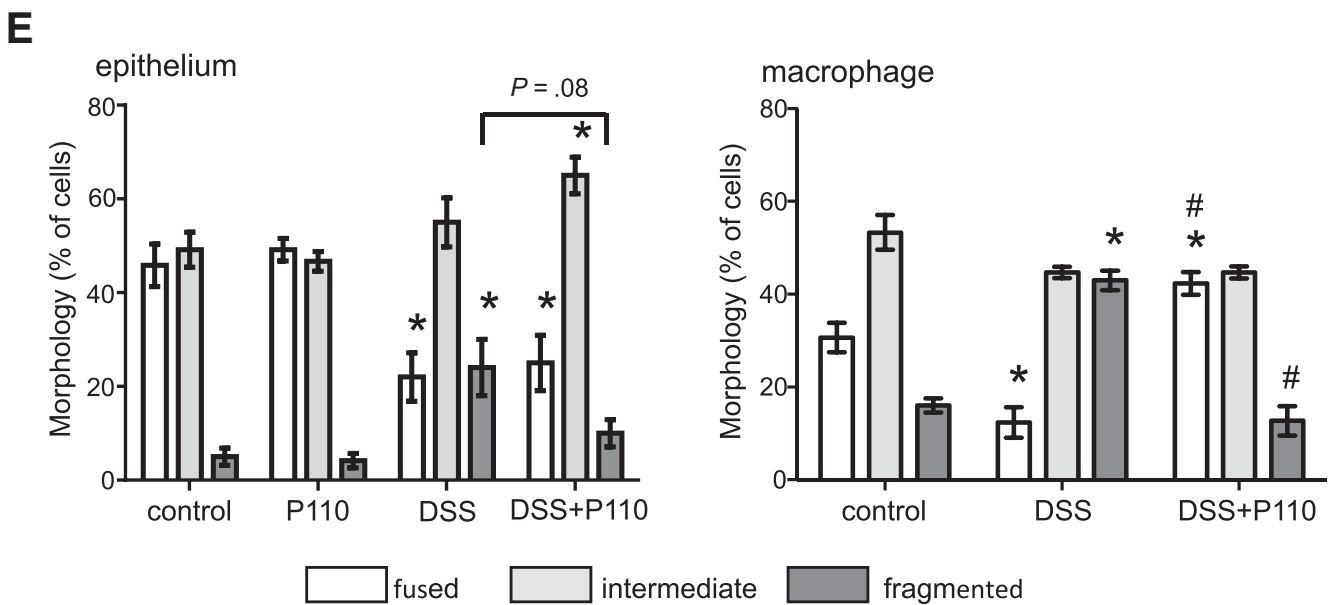
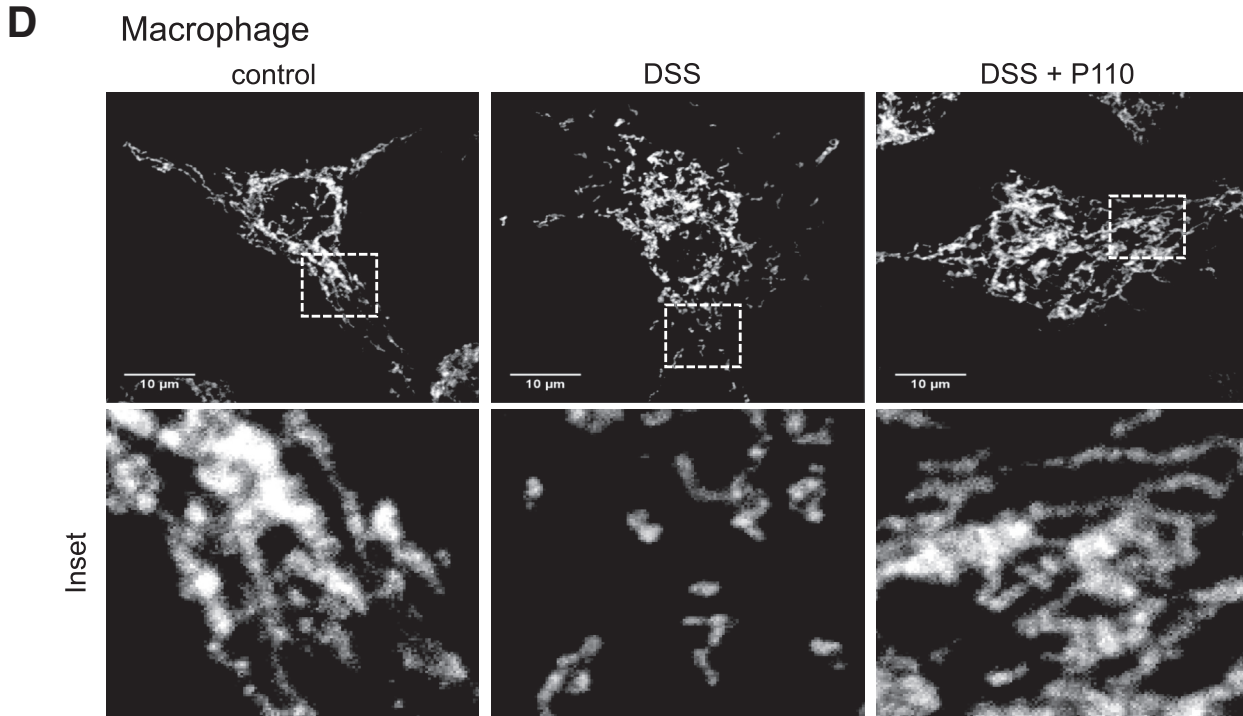


Figure 8. (continued).

with a neuronal effect, which is compatible with the observation that P110 was effective in relieving the severity of disease in animal models of Huntington’s disease.²⁴

Analyses of colonic histopathology revealed damage that was not significantly different between DSS and DSS + P110 groups; however, DNBS-treated mice had less severe histopathology compared with time-matched DNBS-only treated mice, when P110 was used in a prophylactic or a treatment strategy. Complete mucosal healing is the desired

goal of therapy, but it is not unusual for patients to experience symptom relief and have endoscopic or histologic disease.³⁷ Testing of novel therapies in mice can reveal macroscopic improvement concomitant with histopathology.³⁸ Thus, although P110 has anti-colitic effects, reminiscent of its benefits in models of multiple sclerosis and cardiac dysfunction,^{39,40} future studies are needed to determine whether greater mucosal healing can be achieved as a standalone or adjunct therapy in various models of colitis.

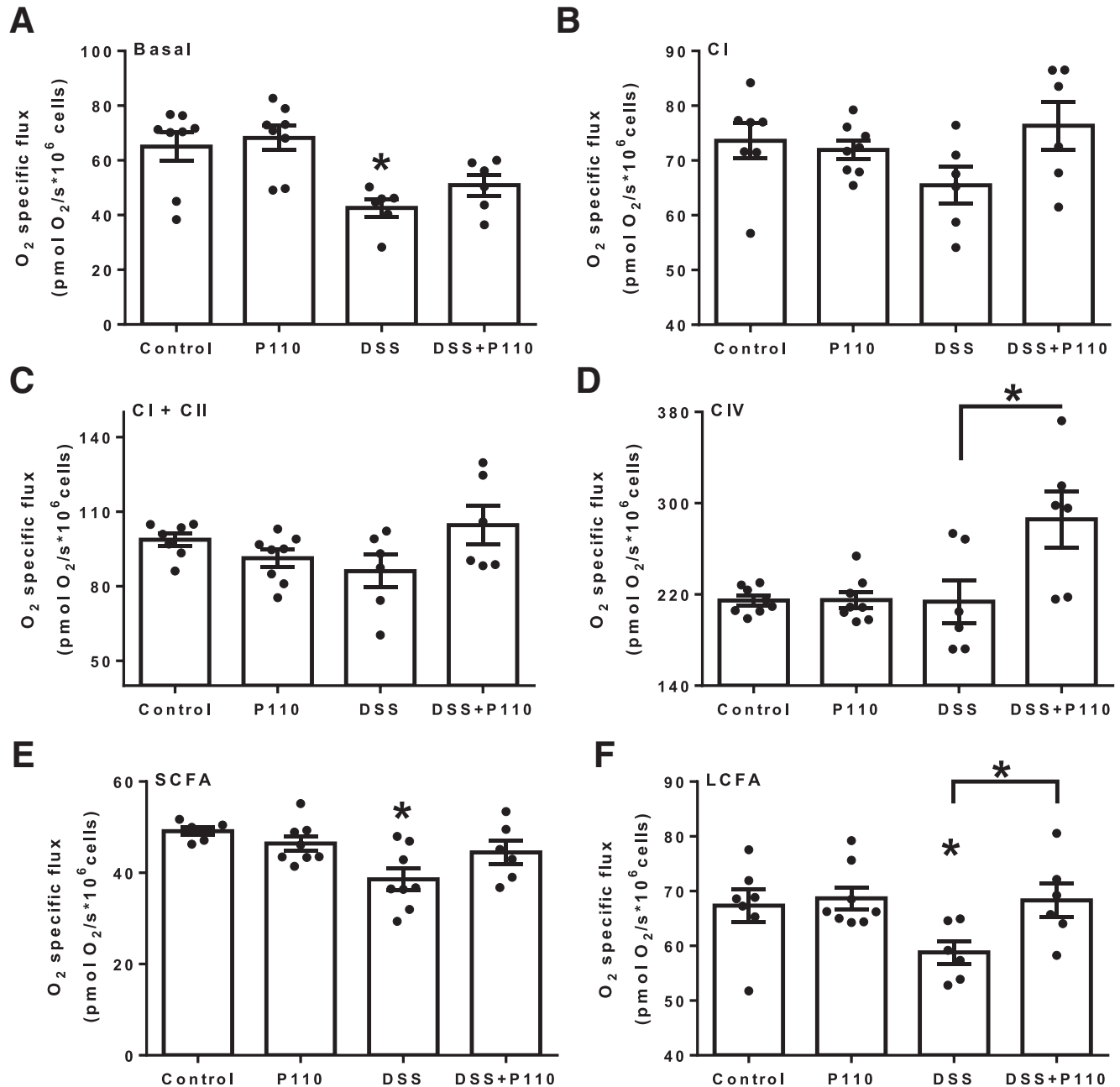


Figure 9. P110 mitigates DSS-induced epithelial mitochondrial respiration defects. Mitochondrial-specific O₂ flux in control, P110 (1.5 μ mol/L, 24 hours), and DSS (2%, 24 hours) \pm P110 in IEC 4.1 cells was determined in the Oxygraph-2K. (A) Changes in oxygen flux are shown for basal respiration of intact cells after permeabilization (Basal), (B–D) for mitochondrial electron transfer chain complexes (CI, CII, CIV), and (E and F) for short-chain (SCFA, butyrate) and long-chain (LCFA, palmitate) fatty acid oxidation. Data are mean \pm standard error of the mean; n = 6–9, epithelial preparations from 2 to 3 experiments; **P* < .05 compared with control; #*P* < .05 compared with DSS; one-way analysis of variance and then Tukey multiple comparison test.

There are challenges in identifying the target cell(s) of an efficacious drug delivered systemically, and so a number of possibilities were pursued.

Microbial dysbiosis is a component of IBD¹³ and murine models of colitis.⁴¹ Fis1 is not expressed in bacteria, but considering the possibility of an off-target, antibacterial effect if P110 entered the gut lumen, assessment of the colonic microbiota was performed. The dysbiosis observed in DSS-

treated mice was unaffected by P110 co-treatment. These data indicate that improvement in disease can occur in advance of correction or normalization of the gut microbiota. Furthermore, P110 treatment did not influence the DSS-evoked increase in circulating neutrophils or the levels of myeloperoxidase activity in tissue extracts (personal observation), suggesting that neutrophils were not the target for P110's anti-colitic effect.

Table 2. Epithelial and Macrophage Cytokine Response to Dextran Sodium Sulfate In Vitro ± Inhibitors of Mitochondrial Fragmentation

	Epithelial KC	Macrophage TNF α	Macrophage IL10
Control	215 ± 25	bd	8 ± 5
P110 (1.5 μ mol/L)	282 ± 15	bd	7 ± 4
Mdivi1 (5 μ mol/L)	265 ± 24	nd	nd
Leflunomide (50 μ mol/L)	241 ± 33	nd	nd
1% DSS	117 ± 12	12 ± 2	58 ± 2
1% DSS + P110	99 ± 3	4 ± 2	86 ± 5 ^a
1% DSS + Mdivi1	58 ± 3	nd	nd
1% DSS + leflunomide	79 ± 12	nd	nd
2% DSS	137 ± 53	28 ± 20	13 ± 8
2% DSS + P110	199 ± 49	33 ± 24	8 ± 5
2% DSS + Mdivi1	154 ± 63	nd	nd
2% DSS + leflunomide	59 ± 19	nd	nd
LPS (10 ng/mL)	3527 ± 187	1740 ± 354	1114 ± 112
LPS + P110	3424 ± 427	2280 ± 450	1037 ± 176

NOTE. The murine small intestinal IEC 4.1 epithelial cell line and M-CSF differentiated murine bone marrow-derived macrophages (2.5×10^5) were stimulated for 24 hours, supernatants were collected, and cytokines were measured by enzyme-linked immunosorbent assay. Data are mean \pm standard error of the mean pg/mL with $n = 4$ and 6 for 1% and 2% DSS, respectively. P110 binds to Fis1 to block mitochondria fission; Mdivi1 inhibits GTPase activity of Drp1 to block mitochondrial fission; leflunomide promotes mitochondria fusion.

bd, below detection limit; KC, keratinocyte chemoattractant; nd, not determined.

^a $P < .05$ compared with 1% DSS only.

Speculating on cell targets for P110, in vitro studies were performed with DSS that can be mucolytic and cytotoxic to the epithelium^{28,42,43} (DNBS' pro-colic effect is by acting as a haptening agent). We confirmed the cytotoxic effect of DSS on a murine gut-derived epithelial cell line, and that DSS can reduce the barrier function of epithelial cell monolayers; neither effect was susceptible to P110 treatment. However, alamarBlue cleavage as an indicator of mitochondrial function suggested that viable enterocytes in the DSS + P110 group were healthier than DSS-only treated cells. In accordance, DSS evoked significant fragmentation of epithelial mitochondria, with corresponding aberrations in energy metabolism (eg, reduced β -oxidation) that were partially negated by P110 co-treatment. Reduced β -oxidation (eg, utilization of butyrate) has been described in ulcerative colitis^{44,45} and was the basis for the hypothesis by Roediger¹⁷ on ulcerative colitis being an energy-deficient disease. Our in vitro data support the postulate that through the ability of P110 to block excessive mitochondrial fission, overall mitochondrial function is enhanced, contributing to reduced disease severity. Extrapolating to the murine models, although P110 did not prevent DSS-induced ulceration (but did in DNBS-treated mice), the surrounding tissue would be healthier, contributing to improvement in the macroscopic clinical signs of disease.

Enteric macrophages are heterogeneous; recently recruited monocytes convert to a macrophage that can drive inflammation, whereas resident macrophages and those of an alternatively activated phenotype promote tissue recovery after injury.^{46–48} DSS may activate macrophages,⁴⁹ and

the finding that DSS evoked mitochondrial network fragmentation in macrophages is novel. The P110 suppression of DSS-induced macrophage mitochondrial fission is compatible with perturbed macrophage mitochondrial dynamics contributing to DSS-colitis. However, suppression of mitochondrial fission in macrophages may reduce efferocytosis,⁵⁰ a component of wound healing, and so further research is necessary to determine the functional consequences of altered macrophage mitochondrial dynamics in IBD.

Immunoneutralization of TNF α is therapeutic in patients. DSS (particularly with LPS) was shown to evoke TNF α from macrophages⁵¹; however, here DSS had a minimal capacity to elicit TNF α or IL10 from murine bone marrow-derived macrophages, and LPS-induced production of these cytokines was unaffected by P110 co-treatment. Thus, we have no data supporting P110 regulation of macrophage-derived cytokine responses as a component of the anti-colic effect, with the exception of a subtle increase in IL10 output from DSS + P110-treated macrophages. It is possible that a small local increase in IL10 evoked by P110 could aid in the suppression of colitis.

Another possibility is that P110 limited the severity of colitis by affecting nerves, and this would align with the absence of hyperalgesia in the DNBS + P110-treated mice. Furthermore, the normalization of colonic motility in P110 + DSS-treated mice is consistent with neuronal regulation, but this could also reflect overall improvement in the gut because of less disease. Neuronal contributions to inflammation and anti-inflammatory reflexes

are well-described, and because of the therapeutic potential of P110 in neurologic disease,²⁵ research efforts should be directed toward determining whether mitochondrial dynamics play a role in the hyperalgesia associated with gastrointestinal disease.

Conclusions

Regulated by complex and coordinated processes, maintaining mitochondrial homeostasis is essential to cellular health. Given this, it is not unexpected that disrupted mitochondrial dynamics (ie, fission and fusion) are implicated in inflammation and the pathogenesis of many diseases. Despite this, there is a paucity of information on these key homeostatic processes in the normal intestine or during inflammation. Addressing this knowledge gap, data are presented to support increased mitochondrial fission as a component of enteric inflammation that can be pharmacologically targeted to reduce disease severity. We suggest that targeting mitochondrial fission is a significant departure from the pursuit of immunomodulators to treat IBD and may represent a novel therapeutic target for IBD management.

Materials and Methods

Ethical Consent

Animal experiments adhered to the Canadian guidelines on animal welfare as administered by the University of Calgary Animal Care Committee protocol AC13-0015.

Real-Time Quantitative Polymerase Chain Reaction

Murine colonic tissue was placed in Ribozol (VWR, Radnor, PA), RNA was extracted, and cDNA synthesis was performed with iScript (Bio-Rad, Mississauga, ON, Canada). Assessment of Drp1, Fis1, OPA1, MFN1, MFN2, and 18S rRNA (used as a housekeeping gene) mRNA expression was performed in the Realplex Eppendorf Mastercycler using iQSYBER Green Supermix (Bio-Rad Laboratories, Hercules, CA) with 625 ng cDNA and the primers shown in Table 3. Resulting values were computed to SYBR green expression on the basis of a standard curve and normalized to 18S rRNA expression. No-template and no-reverse transcription negative controls were used, and melting curves were performed. Assays were performed in triplicate.

Murine fecal samples and cecal contents were collected, and total DNA was extracted from 250 mg fecal/cecal material.⁵² The 16S rRNA gene expression was determined with SYBR green using 20 ng/mL DNA and 0.3 μ mol/L primers (Table 3), and copy numbers were calculated according to available methodology, <http://cels.uri.edu/gsc/cndna.html>. Standard curves were normalized to 16S rRNA by using reference strain genome size and 16S rRNA gene copy number values. Data are expressed as 16S rRNA gene copies/mg fecal/cecal material.⁵³ Principal component analysis was used to compare the microbial signatures between the groups using MetaboAnalyst 4.0.

Induction and Assessment of Colitis

Colitis was induced in 7- to 9-week-old male BALB/c mice (Charles River Labs, Sherbrooke, QC, Canada) with DSS (5%, 40 kDa; Affymetrix, Santa Clara, CA) drinking water for 5 days, then 3 days normal water) or DNBS (3 mg, intrarectal, 72 hours).^{6,49} Animals were weighed and observed daily and humanely killed if they lost >20% weight. At necropsy, the colon was excised and measured, and a macroscopic disease score was calculated.^{6,49} A portion of mid-colon was fixed and paraffin-embedded; sections were collected on coded slides and H&E stained; and histopathology was scored in a blinded fashion on a 0–12 scale.^{6,49} Other sections were immunostained for the proliferation-related antigen Ki67 (1:400 dilution, Abcam ab15580; Abcam, Cambridge, UK), and apoptotic/death/DNA damaged cells were identified in the section by using TUNEL staining and following the manufacturer's recommendations (*In Situ* Cell Death Detection kit, TMR Red; Roche, Basel, Switzerland). P110 (a gift from Dr D. Mochly-Rosen, Stanford University) was administered daily (3 mg/kg, intraperitoneal),²⁴ as depicted in the figures.

Additional 1-cm segments of distal colon were extracted and subjected to a 96-well multiple cytokine protein 14-plex assay in MESO QuickPlex SQ 120 (GM-CSF, interferon- γ , IL2, IL4, IL6, IL9, IL10, IL13, IL17A, IL17F, IL21, IL22, IL25, TNF α) following the manufacturer's instructions (Meso Scale Discovery, Rockville, MD). Data are presented as pg cytokine/10 mg colon tissue.

Peripheral Blood Cell Count

Blood smears were collected on coded slides and stained with Giemsa, and mononuclear cells, neutrophils, and eosinophils were counted.

Colonic Motility

A 2.5-mm glass bead was inserted 2 cm into the colon in an anesthetized mouse, and the time for the bead to appear at the anal verge/be expelled was recorded.⁵⁴

Visceral Hypersensitivity

The visceromotor response to colorectal distention was assessed as previously described.⁵⁵ Two days before colorectal distention, mice were anesthetized, and electrodes were implanted bilaterally into the abdominal external oblique musculature (Bioflex AS-631; Cooner Wire, Chatsworth, CA). Electrodes were exteriorized at the back of the neck and protected by a plastic tube attached to the skin. After a 48-hour recovery, electrodes were connected to a Bio-Amplifier linked to an electromyogram acquisition system (ADInstruments, Colorado Springs, CO). A 10.5-mm-diameter balloon catheter (Fogarty arterial embolectomy catheter, 4F; Vygon, Écouen, France) was inserted into the rectum to a depth of 5 mm, and 10-second distentions were performed at 15–60 mm Hg pressure by inflating the balloon in a stepwise fashion with water (20, 40, 60, and 80 μ L, respectively), with 5-minute rest intervals. The electromyographic activity of the abdominal muscles was recorded, and visceromotor responses were calculated by using

Table 3. Quantitative PCR Primer Sequences Used in This Study

Gene	Forward sequence	Reverse sequence
Mouse		
18S rRNA	ACGCGCGCTACACTGACTGG	CGATCCGAGGGCCTCACTAAACC
Drp1	CTGGATCACGGGACAAGG	GTTGCCTGTTGTTGGTTCCT
Fis1	CCTGATTGATAAGGCCATGAA	ACAGCCAGTCCAATGAGTCC
OPA1	TGACAAACTTAAGGAGGCTGTG	CATTGTGCTGAATAACCCTCAA
MFN1	GTGAGCTTCACCAGTGCAAAA	CACAGTCCGAGCAAAAGTAGTGG
MFN2	CATTCTTGTGGTCGGAGGAG	AAGGAGAGGGCGATGAGTCT
Enteric bacteria		
Bacteroidetes		
<i>Bacteroides/Prevotella</i>	TCCTACGGGAGGCAGCAGT	CCGCACCCACTGTGTTGA
Firmicutes		
<i>Clostridium coccoides (cluster (C) XIV)</i>	ACTCCTACGGGAGGCAGC	GCTTCTTAGTCARGTACCG
<i>Clostridium leptum (C IV)</i>	GCACAAGCAGTGGAGT	CTTCCTCCGTTTGTCAA
<i>Clostridium group (C I)</i>	ATGCAAGTCGAGCGATG	TATGCGGTATTAATCTYCCTTT
<i>Clostridium group (C XI)</i>	ACGCTACTTGAGGAGGA	GAGCCGTAGCCTTTCACT
<i>Lactobacillus</i>	GAGGCAGCAGTAGGGAATCTTC	GGCCAGTTACTACCTCTATCCTTCTT
<i>Roseburia hominus</i>	TACTGCATTGGAACCTGTCCG	CGGCACCGAAGAGCAAT
Actinobacteria		
<i>Bifidobacterium</i>	CGCGTCYGGTGTGAAAG	CCCCACATCCAGCATCCA
Archaea		
<i>Methanobrevibacter</i>	CTCACCGTCAGAATCGTTCAGTC	ACTTGAGATCGGGAGAGGTTAGAGG
Proteobacteria		
<i>Enterobacteriaceae</i>	CATTGACGTTACCCGCAGAAGC	CTCTACGAGACTCAAGCTTGC
Verrucomicrobia		
<i>Akkermansia muciniphila</i>	TCTTCGGAGGCGTTACACAG	AGTTGATCTGGGCAGTCTCG

LabChart 7 software (ADInstruments). Investigators were blinded to the treatment group.

Immunoblotting

Samples of mouse mid-colon were frozen and subsequently homogenized in protein lysis buffer, and protein was quantified by Bradford assay (Bio-Rad). Protein (60 μ g) was loaded into a 12% agarose gel, transferred to a polyvinylidene difluoride membrane (0.2 μ m pore size), and probed for p-Drp1 Ser616 (D9A1, 1:1000; Cell Signaling, Danvers, MA), Drp1 (ab56788, 1:2000; Abcam), and actin (sc-1616 1:1000; Santa Cruz Biotechnology, Santa Cruz, CA). After secondary antibody incubation, washing, and band detection, densitometric analysis was performed on inverted images on ImageJ software (NIH, Bethesda, MD).

Bone Marrow-Derived Macrophages

Bone marrow was flushed from mouse femurs with RPMI 1640 medium (Sigma-Aldrich, St Louis, MO), sieved through a 100- μ m cell strainer, and cultured for 7 days in RPMI containing 10% fetal bovine serum, 2% L-glutamine, 2% penicillin-streptomycin, 1% sodium pyruvate, and 20 ng/mL recombinant mouse M-CSF (R&D Systems Inc, Minneapolis, MN). Cells were rinsed in Dulbecco phosphate-buffered saline (MgCl₂-, CaCl₂-free), and the adherent macrophages were retrieved by using Versene and adjusted to 2.5 \times 10⁵/mL.

Epithelial Cell Function

Viability. The murine IEC 4.1 intestinal epithelial cell line was cultured under standard conditions⁵⁶ until ~70%

confluent by phase-contrast microscopy and treated with 2% DSS \pm P110 (1.5 μ mol/L, 45-minute pretreatment). Twenty-four hours later, cell viability was assessed by trypan blue dye exclusion.

Mitochondrial function. IECs 4.1 (2 \times 10⁴) were seeded into a 96-well plate, and 24 hours later they were treated with 2% DSS \pm P110 (2.5 μ mol/L 45-minute pretreatment, then 1.5 μ mol/L). After 24-hour incubation at 37°C, alamarBlue (1/10 dilution) was added, and 5.5 hours later, recordings were taken at 550 nm (excitation) and 590 nm (emission) by using a SpectraMax i3 (Molecular Devices, San Jose, CA).⁵⁷

Mitochondrial dynamics. Epithelial cells (5 \times 10⁵) were seeded in 8-well chamber slides and stained live with MitoTracker Red CMXRos dye (50 nmol/L; ThermoFisher Scientific, Waltham, MA), followed by Hoescht dye (1 μ g/mL; ThermoFisher), then treated with P110 (45 minutes, 2.5 μ mol/L), followed by 24-hour 2% DSS + P110 (1.5 μ mol/L). Live cells were imaged on the Leica DMI6000B Discovery Flex spinning disk confocal microscope (Leica, Wetzlar, Germany). Bone marrow-derived macrophages were seeded (2.5 \times 10⁵) on sterile coverslips, treated as above, then fixed with 4% paraformaldehyde (PFA), immunolabeled with mouse monoclonal anti-Tom20 antibody (sc-17764; Santa Cruz Biotechnology), and visualized on an Olympus (Tokyo, Japan) spinning disk confocal microscope. The mitochondrial network was quantified for 20 epithelial cells and 50 macrophages/preparation as fused, intermediate, or fragmented morphology expressed as a percent of mitochondrial morphology.⁵⁸

Mitochondrial bioenergetics. Real-time, continuous assessment of oxidative phosphorylation (OXPHOS) in

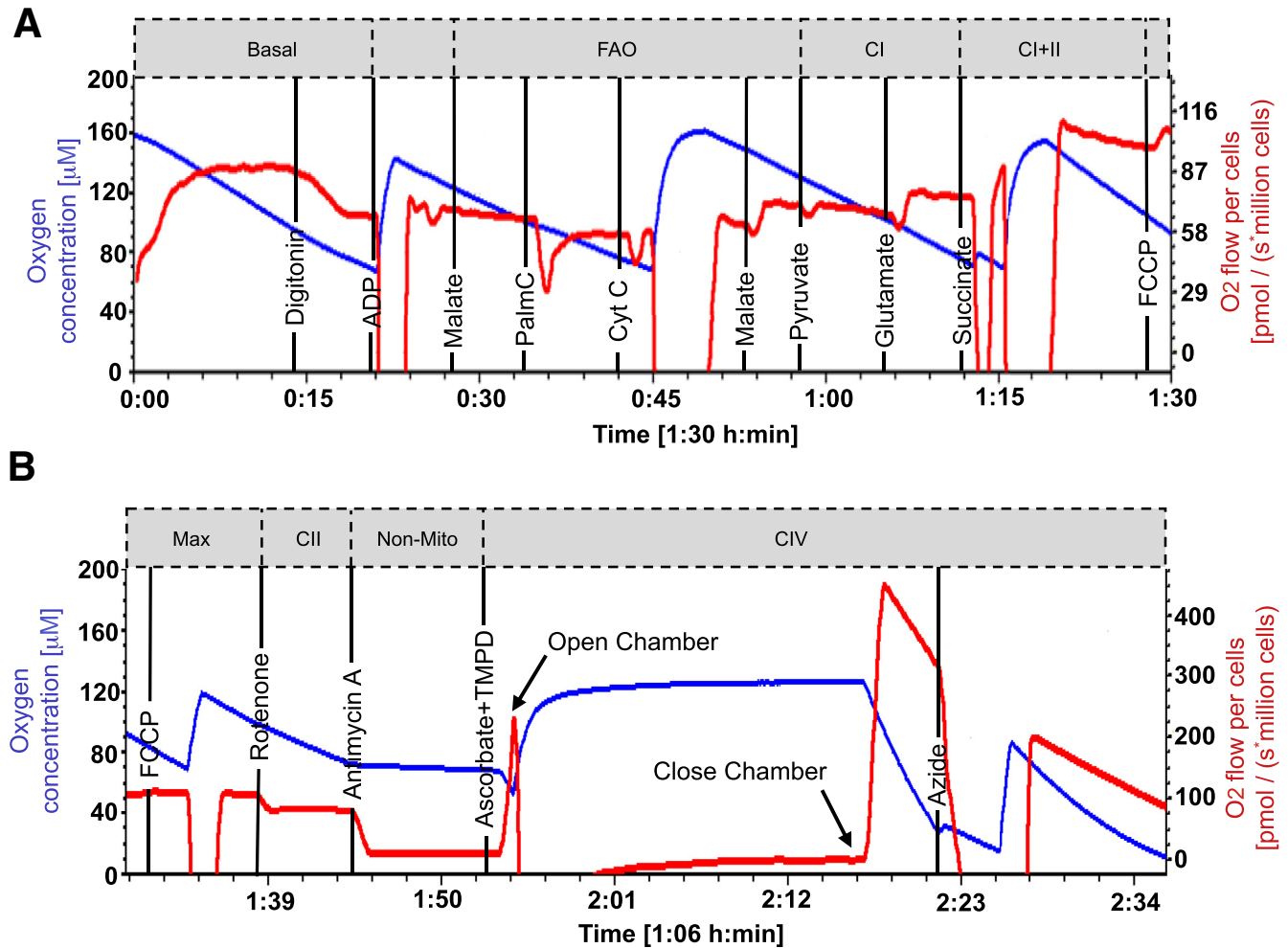


Figure 10. Representative tracings of modified SUIT-002 protocol for analysis of mitochondrial respiration in the murine IEC 4.1 epithelial cell line treated with DSS (2%) \pm P110 (1.5 $\mu\text{mol/L}$). Protocol begins with (A) and continues in (B). Order of substrate addition and specific points of measurement when metabolic pathways are complexes were saturated with substrates are shown (http://www.bioblast.at/index.php/categories_of_SUIT_protocols for additional information). FAO, fatty acid oxidation; Max, maximum oxidative phosphorylation; non-mito, non-mitochondrial respiration.

permeabilized IEC 4.1 cells was performed by using the Oxygraph-2k C-series (Oroboros Instruments, Innsbruck, Austria) according to the substrate inhibitor uncoupler titration protocol-002 with modifications to digitonin and carbonyl cyanide p-(trifluoromethoxy) phenylhydrazone titration protocol (<http://wiki.orooboros.at/index.php/SUIT-002>).⁵⁹ Cells (1.5×10^6) were seeded in 100×20 mm culture dishes for 24 hours, followed by 24-hour exposure to 2% DSS \pm P110 (1.5 $\mu\text{mol/L}$). Cells ($1 \times 10^6/\text{mL}$) were resuspended in mitochondrial respiration medium (MiR05) containing 0.5 mmol/L EGTA, 3 mmol/L $\text{MgCl}_2 \cdot 6\text{H}_2\text{O}$, 20 mmol/L taurine, 10 mmol/L KH_2PO_4 , 20 mmol/L HEPES, 1 g/L bovine serum albumin, 60 mmol/L potassium-lactobionate, and 110 mmol/L sucrose, pH 7.1. On completion of the analysis, cells were collected from the chambers and counted for normalization of oxygen-specific flux. Mitochondrial exclusive respiration was identified by subtracting oxygen consumption in the presence of rotenone (0.5 $\mu\text{mol/L}$) and antimycin A (2.5 $\mu\text{mol/L}$). An additional set of experiments was performed to examine butyrate oxidation in the presence of

adenosine diphosphate (5 mmol/L), sodium butyrate (2 mmol/L), and malate (400 mmol/L) (Figure 10).

Permeability. The human colonic T84 epithelial cell line was cultured on 0.4 μm porous filter supports until electrically confluent at $\geq 1000 \Omega \cdot \text{cm}^6$. Monolayers were then exposed to 2% DSS (apical side) \pm P110, and 24 hours later, epithelial barrier function was assessed by measuring TER with a voltmeter and paired electrodes⁶ (Millipore Sigma, Burlington, MS). Other monolayers were treated with DSS + Z-VAD (20 $\mu\text{mol/L}$, a pan-caspase inhibitor, Cayman Chemical Co, Ann Arbor, MI).

Cytokine Production

Bone marrow-derived macrophages or IEC 4.1 epithelial cells (2.5×10^5) were treated with 1% or 2% DSS or LPS (10 ng/mL) \pm 30-minute pretreatment with P110 (1.5 $\mu\text{mol/L}$),²⁵ Mdivi1 (5 $\mu\text{mol/L}$),⁶⁰ or leflunomide (50 $\mu\text{mol/L}$).³⁶ Twenty-four hours later, culture supernatants were collected, and TNF α , IL10 (macrophages), and keratinocyte

chemoattractant (KC or CXCL1) (epithelium) were measured by enzyme-linked immunosorbent assay (R&D Systems Inc).

Statistical Analysis

Data are presented as means \pm standard error of the mean, where individual dots represent a single mouse. Data are often pooled from multiple experiments, the number of which is defined in the figure legends. For 2-group comparisons, the Student *t* test was applied. Multiple group comparisons of parametric data were by one-way analysis of variance, and when $P < .05$, this was followed by Tukey test or Dunnett multiple comparison test. For nonparametric data, the Kruskal-Wallis test was applied, followed by Dunn test for comparisons to 1 group or Tukey multiple comparison test. A statistically significant difference was accepted when $P < .05$. All analyses were performed with Graph-Pad Prism 6 (GraphPad Software, La Jolla, CA).

References

- Chapman TP, Hadley G, Fratter C, Cullen SN, Bax BE, Bain MD, Sapsford RA, Poulton J, Travis S. Unexplained gastrointestinal symptoms: think mitochondrial disease. *Dig Liver Dis* 2014;46:1–8.
- Patel R, Coulter LL, Rimmer J, Parkes M, Chinnery PF, Swift O. Mitochondrial neurogastrointestinal encephalopathy: a clinicopathological mimic of Crohn's disease. *BMC Gastroenterology* 2019;19:11.
- Nazli A, Yang PC, Jury J, Howe K, Watson JL, Söderholm JD, Sherman PM, Perdue MH, McKay DM. Epithelia under metabolic stress perceive commensal bacteria as a threat. *Am J Pathol* 2004;164:947–957.
- Ho GT, Aird RE, Liu B, Boyapati RK, Kennedy NA, Dorward DA, Noble CL, Shimizu T, Carter RN, Chew ETS, Morton NM, Rossi AG, Sartor RB, Iredale JP, Satsangi J. MDR1 deficiency impairs mitochondrial homeostasis and promotes intestinal inflammation. *Mucosal Immunol* 2018;11:120–130.
- Lewis K, Caldwell J, Phan V, Prescott D, Nazli A, Wang A, Söderholm JD, Perdue MH, Sherman PM, McKay DM. Decreased epithelial barrier function evoked by exposure to metabolic stress and nonpathogenic *E. coli* is enhanced by TNF- α . *Am J Physiol Gastrointest Liver Physiol* 2008;294:G669–G678.
- Wang A, Keita ÅV, Phan V, McKay CM, Schoultz I, Lee J, Murphy MP, Fernando M, Ronaghan N, Balce D, Yates RM, Dickey M, Beck PL, MacNaughton WK, Söderholm JD, McKay DM. Targeting mitochondria-derived reactive oxygen species to reduce epithelial barrier dysfunction and colitis. *Am J Pathol* 2014;184:2516–2527.
- Rath E, Berger E, Messlik A, Nunes T, Liu B, Kim SC, Hoogenraad N, Sans M, Sartor RB, Haller D. Induction of dsRNA-activated protein kinase links mitochondrial unfolded protein response to the pathogenesis of intestinal inflammation. *Gut* 2012;61:1269–1278.
- Yeganeh PR, Leahy J, Spahis S, Patey N, Desjardins Y, Roy D, Delvin E, Garofalo C, Leduc-Gaudet JP, St Pierre D, Beaulieu JF, Murette A, Gouspillou G, Levy E. Apple peel polyphenols reduce mitochondrial dysfunction in mice with DSS-induced ulcerative colitis. *J Nutr Biochem* 2018;57:56–66.
- Söderholm JD, Olaison G, Peterson KH, Franzen LE, Lindmark T, Wiren M, Tagesson C, Sjö Dahl R. Augmented increase in tight junction permeability by luminal stimuli in the non-inflamed ileum of Crohn's disease. *Gut* 2002;50:307–313.
- Amrouche-Mekkioui I, Djerdjouri B. N-acetylcysteine improves redox status, mitochondrial dysfunction, mucin-depleted crypts and epithelial hyperplasia in dextran sulfate sodium-induced oxidative colitis in mice. *Eur J Pharmacol* 2012;691:209–217.
- Schurmann G, Bruwer M, Klotz A, Schmid KW, Senninger N, Zimmer KP. Transepithelial transport processes at the intestinal mucosa in inflammatory bowel disease. *Int J Colorectal Dis* 1999;14:41–46.
- Santhanam S, Rajamanickam S, Motamarry A, Ramakrishna BS, Amirtharaj JG, Ramachandran A, Pulimood A, Venkatraman A. Mitochondrial electron transport chain complex dysfunction in the colonic mucosa in ulcerative colitis. *Inflamm Bowel Dis* 2012;18:2158–2168.
- Chu H, Khosravi A, Kusumawardhani IP, Kwon AH, Vasconcelos AC, Cunha LD, Mayer AE, Shen Y, Wu WL, Kambal A, Targan SR, Xavier RJ, Ernst PB, Green DR, McGovern DP, Virgin HW, Mazmanian SK. Gene-microbiota interactions contribute to the pathogenesis of inflammatory bowel disease. *Science* 2016;352:1116–1120.
- Schoultz I, Soderholm JD, McKay DM. Is metabolic stress a common denominator in inflammatory bowel disease? *Inflamm Bowel Dis* 2011;17:2008–2018.
- Zareie M, Riff J, Donato K, McKay DM, Perdue MH, Söderholm JD, Karmali M, Cohen MB, Hawkins J, Sherman PM. Novel effects of the prototype translocating *Escherichia coli*, strain C25 on intestinal epithelial structure and barrier function. *Cell Microbiol* 2005;7:1782–1797.
- Ma C, Wickham ME, Guttman JA, Deng W, Walker J, Madsen KL, Jacobson K, Vogl WA, Finlay BB, Vallance BA. *Citrobacter rodentium* infection causes both mitochondrial dysfunction and intestinal epithelial barrier disruption *in vivo*: role of mitochondrial associated protein (map). *Cell Microbiol* 2006;8:1669–1686.
- Roediger WE. The colonic epithelium in ulcerative colitis: an energy-deficiency disease? *Lancet* 1980;2:712–715.
- Haberman Y, Karns R, Dexheimer PJ, Schirmer M, Somekh J, Jurickova I, Braun T, Bauman L, Collins MH, Mo A, Rosen MJ, Bankowski E, Gotman N, Marquis J, Nistel M, Rufo PA, Baker SS, Sauer CG, Markowitz J, Pfefferkorn MD, Rosh JR, Boyle BM, Mack DR, Baldassano RN, Shah S, Leleiko NS, Heyman MB, Griffiths AM, Patel AS, Noe JD, Aronow BJ, Kugathasan S, Walters TD, Gibson G, Thomas SD, Mollen K, Shen-Orr S, Huttenhower C, Xavier RJ, Hyams JS, Denson LA. Ulcerative colitis mucosal transcriptomes reveal mitochondrial pathology and personalized mechanisms underlying disease severity and treatment response. *Nat Commun* 2019;10:38.

19. Pernas L, Scorrano L. Mito-Morphosis: mitochondrial fusion, fission, and cristae remodeling as key mediators of cellular function. *Ann Rev Physiol* 2016;78:505–531.
20. Eisner V, Picard M, Hajnoczky G. Mitochondrial dynamics in adaptive and maladaptive cellular stress responses. *Nat Cell Biol* 2018;20:755–765.
21. Osellame LD, Singh AP, Stroud DA, Palmer CS, Stojanovski D, Ramachandran R, Ryan MT. Cooperative and independent roles of the Drp1 adaptors Mff, MiD49 and MiD51 in mitochondrial fission. *J Cell Sci* 2016;129:2170–2181.
22. Ryan J, Dasgupta A, Huston J, Chen KH, Archer SL. Mitochondrial dynamics in pulmonary arterial hypertension. *J Mol Med* 2015;93:229–242.
23. Archer SL. Mitochondrial dynamics: mitochondrial fission and fusion in human diseases. *N Engl J Med* 2013;369:2236–2251.
24. Guo X, Disatnik MH, Monbureau M, Shamloo M, Mochly-Rosen D, Qi X. Inhibition of mitochondrial fragmentation diminishes Huntington's disease-associated neurodegeneration. *J Clin Invest* 2013;123:5371–5388.
25. Qi X, Qvit N, Su YC, Mochly-Rosen D. A novel Drp1 inhibitor diminishes aberrant mitochondrial fission and neurotoxicity. *J Cell Sci* 2013;126:789–802.
26. Hunter MM, Wang A, Hirota CL, McKay DM. Neutralizing anti-IL-10 antibody blocks the protective effect of tapeworm infection in a murine model of chemically induced colitis. *J Immunol* 2005;174:7368–7375.
27. Boue J, Basso L, Cenac N, Blanpied C, Rollid-derkinderen M, Neunlist M, Vergnolle N, Dietrich G. Endogenous regulation of visceral pain via production of opioids by colitogenic CD4⁺ T cells in mice. *Gastroenterology* 2014;146:166–175.
28. Ni J, Chen SF, Hollander D. Effects of dextran sulphate sodium on intestinal epithelial cells and intestinal lymphocytes. *Gut* 1996;39:234–241.
29. Reinglas J, Gonczi L, Kurt Z, Bessisow T, Lakatos PL. Positioning of old and new biologicals and small molecules in the treatment of inflammatory bowel diseases. *World J Gastroenterol* 2018;24:3567–3582.
30. Novak EA, Mollen KP. Mitochondrial dysfunction in inflammatory bowel disease. *Front Cell Dev Biol* 2015;3:62.
31. Rath E, Moschetta A, Haller D. Mitochondrial function: gatekeeper of intestinal epithelial cell homeostasis. *Nat Rev Gastroenterol Hepatol* 2018;15:497–516.
32. Mottawea W, Chiang CK, Muhlbauer M, Starr AE, Butcher J, Abujamel T, Deeke SA, Brandel A, Zhou H, Shikralla S, Hajjibabaei M, Singleton R, Benchimol E, Jobin C, Mack DR, Figeys D, Stintzi A. Altered intestinal microbiota-host mitochondria crosstalk in new onset Crohn's disease. *Nat Commun* 2016;7:13419.
33. Wang SQ, Cui SX, Qu XJ. Metformin inhibited colitis and colitis-associated cancer (CAC) through protecting mitochondrial structures of colorectal epithelial cells in mice. *Cancer Biol Ther* 2018;1–11.
34. Bou-Fersen AM, Anim JT, Khan I. Experimental colitis is associated with ultrastructural changes in inflamed and uninfamed regions of the gastrointestinal tract. *Med Princ Practice* 2008;17:190–196.
35. Bordt EA, Clerc P, Roelofs BA, Saladino AJ, Tretter L, Adam-Vizi V, Cherok E, Khalil A, Yadava N, Ge SX, Francis TC, Kennedy NW, Picton LK, Kumar T, Uppuluri S, Miller AM, Itoh K, Karbowski M, Sesaki H, Hill RB, Polster BM. The putative Drp1 inhibitor Mdivi-1 is a reversible mitochondrial complex I inhibitor that modulates reactive oxygen species. *Dev Cell* 2017;40:583–594.
36. Miret-Casals L, Sebastian D, Brea J, Rico-Leo EM, Palacin M, Fernandez-Salguero PM, Loza MI, Albericio F, Zorzano A. Identification of new activators of mitochondrial fusion reveals a link between mitochondrial morphology and pyrimidine metabolism. *Cell Chem Biol* 2018;25:268–278.
37. Osterman MT. Mucosal healing in inflammatory bowel disease. *J Clin Gastroenterol* 2013;47:212–221.
38. Reardon C, Sanchez A, Hogaboam CM, McKay DM. Tapeworm infection reduces epithelial ion transport abnormalities in murine dextran sulfate sodium-induced colitis. *Infect Immun* 2001;69:4417–4423.
39. Disatnik MH, Ferreira JC, Campos JC, Gomes KS, Dourado PM, Qi X, Mochly-Rosen D. Acute inhibition of excessive mitochondrial fission after myocardial infarction prevents long-term cardiac dysfunction. *J Am Heart Assoc* 2013;2:e000461.
40. Luo F, Herrup K, Qi X, Yang Y. Inhibition of Drp1 hyperactivation is protective in animal models of experimental multiple sclerosis. *Exp Neurol* 2017;292:21–34.
41. Darnaud M, Dos Santos A, Gonzalez P, Augui S, Lacoste C, Desterke C, De Hertogh G, Valentino E, Braun E, Zheng J, Biosgard R, Neut C, Dubuquoy L, Chiappini F, Samuel D, Lepage P, Guerrieri F, Dore J, Brechot C, Moniaux N, Faivre J. Enteric delivery of regenerating family member 3 alpha alters the intestinal microbiota and controls inflammation in mice with colitis. *Gastroenterology* 2018;154:1009–1023.
42. Dieleman LA, Ridwan BU, Tennyson GS, Beagley KW, Bucy RP, Elson CO. Dextran sulfate sodium-induced colitis occurs in severe combined immunodeficient mice. *Gastroenterology* 1994;107:1643–1652.
43. Johansson ME, Gustafsson JK, Holmen-Larsson J, Jabbar KS, Xia L, Xu H, Ghisham F, Carvalho FA, Gewirtz AT, Sjoval H, Hansson GC. Bacteria penetrate the normally impenetrable inner colon mucus layer in both murine colitis models and patients with ulcerative colitis. *Gut* 2014;63:281–291.
44. Chapman MA, Grahn MF, Boyle MA, Hutton M, Rogers J, Williams NS. Butyrate oxidation is impaired in the colonic mucosa of sufferers of quiescent ulcerative colitis. *Gut* 1994;35:73–76.
45. De Preter V, Arijis I, Windey K, Vanhove W, Vermeire S, Schuit F, Rugeerts P, Verbeke K. Impaired butyrate oxidation in ulcerative colitis is due to decreased butyrate uptake and a defect in the oxidation pathway. *Inflamm Bowel Dis* 2012;18:1127–1136.
46. Rugtveit J, Nilsen EM, Bakka A, Carlsen H, Brandtzaeg P, Scott H. Cytokine profiles differ in newly recruited and resident subsets of mucosal macrophages from inflammatory bowel disease. *Gastroenterology* 1997;112:1493–1505.

47. Schleier L, Wiendl M, Heidbreder K, Binder MT, Atreya R, Rath T, Becker E, Schulz-Kuhnt A, Stahl A, Schulze LL, Ullrich K, Merz SF, Bornemann L, Gunzer M, Watson AJM, Neufert C, Atreya I, Neurath MF, Zundler S. Non-classical monocyte homing to the gut via $\alpha 4\beta 7$ integrin mediates macrophage-dependent intestinal wound healing. *Gut* 2020;69:252–263.
48. Minutti CM, Knipper JA, Allen JE, Zaiss DM. Tissue-specific contribution of macrophages to wound healing. *Semin Cell Dev Biol* 2017;61:3–11.
49. Arai T, Lopes F, Shute A, Wang A, McKay DM. Young mice expel the tapeworm *Hymenolepis diminuta* and are protected from colitis by triggering a memory response with worm antigen. *Am J Physiol Gastrointest Liver Physiol* 2018;314:G461–G470.
50. Wang Y, Subramanian M, Yurdagul A Jr, Barbosa-Lorenzi VC, Cai B, de Juan-Sanz J, Rayan TA, Nomura M, Maxfield FR, Tabas I. Mitochondrial fission promotes the continued clearance of apoptotic cells by macrophages. *Cell* 2017;171:331–345.
51. Kono Y, Miyoshi S, Fujita T. Dextran sodium sulfate alters cytokine production in macrophages in vitro. *Die Pharmazie* 2016;71:619–624.
52. Bomhof MR, Saha DC, Reid DT, Paul HA, Reimer RA. Combined effects of oligofructose and *Bifidobacterium animalis* on gut microbiota and glycemia in obese rats. *Obesity* 2014;22:763–771.
53. Stoddard SF, Smith BJ, Hein R, Roller BR, Schmidt TM. rrnDB: improved tools for interpreting rRNA gene abundance in bacteria and archaea and a new foundation for future development. *Nucleic Acids Res* 2015;43:D593–D598.
54. Storr MA, Bashashati M, Hirota C, Vemuri VK, Keenan CM, Duncan M, Lutz B, Makie K, Makriyannis A, MacNaughton WK, Sharkey KA. Differential effects of CB(1) neutral antagonists and inverse agonists on gastrointestinal motility in mice. *Neurogastroenterol Motil* 2010;22:787–796.
55. Esquerre N, Basso L, Dubuquoy C, Djouina M, Chappard D, Blanpied C, Desreumaux P, Vergnolle N, Vignal C, Body-Malapel M. Aluminum ingestion promotes colorectal hypersensitivity in rodents. *Cell Mol Gastroenterol Hepatol* 2019;7:185–196.
56. Lopes F, Reyes JL, Wang A, Leung G, McKay DM. Enteric epithelial cells support growth of *Hymenolepis diminuta* in vitro and trigger TH2-promoting events in a species-specific manner. *Int J Parasitol* 2015;45:691–696.
57. O'Brien J, Wilson I, Orton T, Pognan F. Investigation of the Alamar Blue (resazurin) fluorescent dye for the assessment of mammalian cell cytotoxicity. *Eur J Biochem* 2000;267:5421–5426.
58. Chatel-Chaix L, Cortese M, Romero-Brey I, Bender S, Neufeldt CJ, Fischl W, Scaturro P, Schieber N, Schwab Y, Fischer B, Ruggieri A, Bartenschlager R. Dengue virus perturbs mitochondrial morphodynamics to dampen innate immune responses. *Cell Host Microbe* 2016;20:342–356.
59. Doerrier C, Garcia JA, Volt H, Diaz-Casado ME, Lima-Cabello E, Ortiz F, Luna-Sanchez M, Escames G, Lopez LC, Acuna-Castoviejo D. Identification of mitochondrial deficits and melatonin targets in liver of septic mice by high-resolution respirometry. *Life Sci* 2015;121:158–165.
60. Smith G, Gallo G. To mdivi-1 or not to mdivi-1: is that the question? *Dev Neurobiol* 2017;77:1260–1268.

Received October 28, 2019. Accepted April 6, 2020.

Correspondence

Address correspondence to: Derek M. McKay, PhD, Department of Physiology and Pharmacology, 1877 HSC, University of Calgary, 3330 Hospital Drive NW, Calgary, Alberta, Canada T2N 4N1. e-mail: dmckay@ucalgary.ca; fax: (403) 283-3029.

Acknowledgments

N. Mancini was a recipient of University of Calgary Eyes High, Killam and Natural Sciences and Engineering Research Council of Canada (NSERC) studentships, and L. Goudie an NSERC studentship. T. Jayme was supported by a studentship from the NSERC CREATE in Host-Parasite Interactions (HPI) Program at University of Calgary. E. van Tilburg Bernardes is funded by an Eyes High Doctoral Scholarship (University of Calgary). D. M. McKay holds a Canada Research Chair (Tier 1) in Intestinal Immunophysiology in Health and Disease. The authors thank Ms C. MacNaughton (University of Calgary) for instruction in the colonic motility assay. Dr Rajabi's current address is Health Sciences Department, College of Natural and Health Sciences, Zayed University, Abu Dhabi, UAE.

Author contributions

NLM: study concept and design; acquisition of data; analysis and interpretation of data; drafting of the manuscript; critical revision of the manuscript for important intellectual content; statistical analysis. LG: study concept and design; acquisition of data; analysis and interpretation of data; drafting of the manuscript; statistical analysis. WX: acquisition of data. RS: acquisition of data; analysis and interpretation of data; critical revision of the manuscript for important intellectual content; statistical analysis. SR: acquisition of data; analysis and interpretation of data; critical revision of the manuscript for important intellectual content; statistical analysis. AW: acquisition of data; analysis and interpretation of data. NE: acquisition of data; analysis and interpretation of data; critical revision of the manuscript for important intellectual content; statistical analysis. AAR: acquisition of data; analysis and interpretation of data; critical revision of the manuscript for important intellectual content. TSJ: acquisition of data; analysis and interpretation of data. YN: analysis and interpretation of data; critical revision of the manuscript for important intellectual content. EVTB: acquisition of data; critical revision of the manuscript for intellectual content. JGPF: analysis and interpretation of data; critical revision of the manuscript for important intellectual content. TS: analysis and interpretation of data; critical revision of the manuscript for important intellectual content. JS: study concept and design; analysis and interpretation of data; drafting of the manuscript; critical revision of the manuscript for important intellectual content; obtained funding; study supervision. DMM: study concept and design; analysis and interpretation of data; drafting of the manuscript; critical revision of the manuscript for important intellectual content; obtained funding; study supervision.

Conflicts of interest

The authors disclose no conflicts.

Funding

Supported by an Innovation Grant from Crohn's Colitis Canada (J.S., D.M.M) and a grant from the Canadian Institutes for Health Research (D.M.M).